DISCLAIMER NOTICE

THIS DOCUMENT IS BEST QUALITY PRACTICABLE. THE COPY FURNISHED TO DTIC CONTAINED A SIGNIFICANT NUMBER OF PAGES WHICH DO NOT REPRODUCE LEGIBLY.

Final Report

ELECTRICAL EFFECTS OF SHOCK WAVES:

CONDUCTIVITY IN CsI AND KI. THERMOELECTRIC MEASUREMENTS IN METALS

Prepared for:

BALLISTIC RESEARCH LABORATORIES
ABERDEEN PROVING GROUND
MARYLAND

CONTRACT DA-04-200-ORD-1279

August 31, 1963

Final Report

ELECTRICAL EFFECTS OF SHOCK WAVES:

CONDUCTIVITY IN CsI AND KI. THERMOELECTRIC MEASUREMENTS IN METALS

Prepared for:

BALLISTIC RESEARCH LABORATORIES
ABERDEEN PROVING GROUND
MARYLAND

CONTRACT DA-04-200-ORD-1279

By: D. G. Doran T. J. Ahrens
Poulter Laboratories

SRI Project No. PGU-4100

Approved:

G. E. DUVALL, DIRECTOR
POULTER LABORATORIES

Copy No. 5

ABSTRACT

Incidence of a 400 kb shock wave in copper upon a constantan probe produces a peak emf of the order of 80 mv, compared with 14 mv calculated from zero-pressure thermopowers and theoretical shock temperatures. At 170 kb, measured peak emfs range from 23 to 90 mv, compared with 4 mv calculated similarly. The signals decrease by 50% during the first 0.1 to 0.3 μsec, followed by a much less rapid decrease. Partial diffusion welding of the junction reduces the initial spike at 400 kb. Varying the probe diameter from $\frac{1}{8}$ inch to $\frac{3}{4}$ inch only slightly affects the signal. Anomalously high emfs are also observed with aluminum-constantan, copper-iron, and copper-aluminum junctions. Signal amplitudes are related approximately as they would be at zero pressure, with the exception of copper-iron in which the iron is known to undergo a phase transition.

Electrical resistivities of single-crystal NaCl, KI, and CsI have been measured at several shock pressures in the range 84 to 274 kb. The resistivity of NaCl is greater than 4×10^5 ohm-cm at 231 kb, in disagreement with both Alder (*Solids Under Pressure*, McGraw Hill, N.Y., 1963, pp. 385-420) and Al'tshuler *et al.*, [*Soviet Physics JETP, 12,* 10-15 (1961)]. The resistivity of KI is greater than 2×10^5 ohm-cm at 93 kb, but drops to less than 1 ohm-cm at 233 kb. The resistivity of CsI is greater than 6×10^5 ohm-cm at 215 kb, and less than 25 ohm-cm at 274 kb. Agreement with Alder for CsI and KI is semiquantitative. It is believed that the decreased resistivity is due to an ionic or electronic mechanism rather than a polymorphic transition. Resistivity measurements were performed parallel (longitudinal geometry) and perpendicular (transverse geometry) to the shock propagation direction; the above values are for longitudinal geometry. The few measurements in transverse geometry indicate lower resistivities, particularly for KI.

In longitudinal geometry a signal is produced during shock transit which, if the shocked specimen resistivity is high, is independent of applied voltage and is qualitatively similar to that observed in insulators by Hauver [ONR Symposium Report ACR-52, Vol. 1, 241-252 (1960)]. If the

resistivity of the shocked material is low, the signal observed is not that predicted on the basis of low resistivity alone. One transverse experiment in CsI, with no applied field, prcduced a signal during shock transit contrary to expectations.

FOREWORD

The purpose of this project is to study electrical effects associated with the propagation of shock waves in solids. In the past few years, other laboratories have studied several shock-induced electrical effects including the depolarization of ferroelectric ceramics, the conductivity of sulfur and other materials, and the polarization of certain materials. The motivation for some of this work has been the search for explosive-electric and pressure-electric transducers.

Basic study of some of the above phenomena should produce data and insight concerning the fundamentals of the shock process itself and should also provide tools for the study of the changes induced in solids by shock waves. It is obvious, however, that a project of modest size must concentrate its efforts on a few specific areas of interest if it is not to be completely exploratory in nature. There is indeed considerable incentive for exploratory research--the need for diagnostic tools for pressure and temperature measurement, the need to avoid spurious electrical effects in present electrical measurements utilizing circuit elements which are shocked in the course of the measurement, and, of course, scientific curiosity.

Our initial efforts have been directed toward one exploratory problem and one more-straightforward problem. The first concerns an observation made at Stanford Research Institute,[1] Los Alamos Scientific Laboratory,[2] and the University of Poitiers, the latter work being the subject of recent papers by J. Jacquesson.[3]* In each case an attempt was made to measure shock temperatures in copper and iron specimens by using constantan probes to produce a thermoelectric voltage. Also in each case, the observed signal was many times the signal expected on the basis of atmospheric pressure thermopowers and calculated shock temperatures. Jacquesson has shown that the signal produced with his experimental arrangement decreases monotonically with decreasing shock pressure, and

* A Russian paper on this subject was published after the present study began. See Ref. 4.

apparently he believes it to be primarily pressure sensitive. He offers no explanation for the effect. It seems clear, because of the unexpected and unexplained magnitude of the signal and because of the need for effects which have known pressure and temperature sensitivities, that this effect is worthy of further study.

The more-straightforward problem referred to is that of resistance measurement under shock loading. It is straightforward only in the sense that we know what we are looking for. Resistance measurements of shocked solids have been reported by Alder and Christian[5] (alkali halides, I_2, red phosphorus, $LiAlH_4$), Brish, Tarasov, and Tsukerman[6] (plexiglas, paraffin), David and Hamman[7] (sulfur), Joigneau and Thouvenin[8] (sulfur), Hauver[9] (sulfur), Al'tshuler, Kuleshova, and Pavlovskii[10] (NaCl), and Fuller and Price[11] (manganin, iron). We have concerned ourselves with the problem of measuring the change of resistance produced by shock loading materials which are insulators at atmospheric pressure, concentrating on the alkali halides, NaCl, KI, and CsI. The decrease of resistivity with pressure may be continuous (though possibly very rapid) as in the gradual narrowing of the gap between valence and conduction bands with ultimate overlap, or may be abrupt as in the case of an electronic or crystallographic transition. Drickamer[12] has made static measurements on KI and CsI to 400-500 kb with no evidence of transition to a conducting state,* whereas Alder and Christian have reported[5] resistivities of the order of 100 ohm-cm in the same materials shocked to 200 kb. This suggests that the shock-induced conductivity is not the result of pressure alone, but is due to the high temperature of the shocked material and/or effects present in shock compression, such as the production of crystal defects, nonhydrostatic stress distribution, etc.

* It should be pointed out that this is based on a negative experimental result in that no resistance measurement is possible in the apparatus unless the specimen resistance is less than about 10^7 ohms.

CONTENTS

ABSTRACT ii

FOREWORD iv

LIST OF ILLUSTRATIONS. vii

LIST OF TABLES ix

I ANOMALOUS THERMOELECTRIC EFFECT. 1
- A. Introduction 1
- B. Experimental Program 3
- C. Discussion 13

II ELECTRICAL RESISTIVITY 18
- A. Introduction 18
- B. Experimental Techniques. 19
  - 1. Time Correlation Between Shock Wave Position and Oscilloscope Trace 21
  - 2. Longitudinal Configuration 22
  - 3. Transverse Configuration 26
  - 4. Specimen Preparation 28
- C. Experimental Results 29
  - 1. Alkali Halide Resistivity. 29
  - 2. Charge Generation. 36
  - 3. Resistivity of Some Insulating Materials 39
  - 4. Shock Velocities and Determination of Shocked States 39
- D. Discussion 41
- E. Conclusions. 45

APPENDIX A DETERMINATION OF RESISTIVITY FROM A TRANSVERSE GEOMETRY EXPERIMENT 46

APPENDIX B A VARIABLE CAPACITOR MODEL OF A SPECIMEN IN A LONGITUDINAL GEOMETRY EXPERIMENT. 50

ACKNOWLEDGMENTS. 56

REFERENCES 57

ILLUSTRATIONS

Fig. 1 Block Diagram of Recording Circuits Used for Shot 8683 5

Fig. 2 Schematic Diagram of Shot 8683 6

Fig. 3 Signal from Cu-Constantan Junction in Shot 8682. 7

Fig. 4 Signals from Cu-Al Junction and from Cu-Constantan Junction in Shot 8683. 7

Fig. 5 Signal from Cu-Cu Junction and from Cu-Fe Junction in Shot 8683 8

Fig. 6 Probe Arrangement for Shots 8745 and 8746. 9

Fig. 7 Experimental Arrangement for Shots 8889 and 8890 9

Fig. 8 Signals Observed in Shot Geometry of Fig. 7. 10

Fig. 9 Assembly for Shots 9145 and 9146 12

Fig. 10 Signals from Shots 9145 and 9146 12

Fig. 11 Signals from Thermoelectric Shots. 14

Fig. 12 Electronic Arrangement for Shock Resistivity Measurements. 20

Fig. 13 Longitudinal Configuration—Electrical Resistivity Measurement in Shock-Propagation Direction 23

Fig. 14 Polarization Signal for NaCl at 231 kb—Shot 9483. 23

Fig. 15 (a) Conduction Signal for KI at 181 kb—Shot 9505
(b) Polarization, Followed by Conduction Signal—Shot 9498 24

Fig. 16 Longitudinal Configuration—Shock Resistivity Measurement with Photoelectric Detection of Shock Arrival at Specimen-Backing Electrode Interface. 25

Fig. 17 Framing Camera Sequence Showing Shock in Aluminum Driver Plate Impinging on NaCl Crystal Surrounded by Air. 26

Fig. 18 Transverse Configuration—Resistivity Measurement Perpendicular to Direction of Shock Propagation. 27

Fig. 19 Pressure *vs.* Particle Velocity for Various Insulators. 28

Fig. 20 Resistivity *vs.* Relative Volume and Shock Temperature for CsI. 30

Fig. 21 Resistivity *vs.* Relative Volume and Shock Temperature for KI 31

Fig. 22 Polarization Signal Followed by Steady Conduction Signal—Longitudinal Geometry, Shot 9487 35

Fig. 23 Polarization Signal Corresponding to Entrance and Exit of Shock Front in Silicone Oil at 106 kb—Shot 9504 37

Fig. 24 Polarization Signal for CsI at 107 kb—Shot 9382 37

Fig. 25 Polarization Signal and Small Conduction Signal for CsI at 215 kb—Shot 9499 38

ILLUSTRATIONS

Fig. 2b Polarization Signal in Passive Experiment with CsI at 274 kb--Shot 9380 38

Fig. A-1 Conduction Signal for CsI at 215 kb—Transverse Geometry, Shot 9517. 43

Fig. A-2 Parameters Describing Stress, Volume, and Resistivity in Reflected State Achieved in Transverse Geometry Experiment 48

Fig. B-1 Circuit Schematic Appropriate to Variable Capacitor Model of Shocked Specimen. 51

Fig. B-2 Current *vs.* Time for Variable Capacitor Model of KI at 233 kb 55

TABLES

Table I Thermoelectric Experiments 4

Table II Alkali Halide Resistivity, Longitudinal Geometry 32

Table III Alkali Halide Resistivity, Transverse Geometry 34

Table IV Insulation Test Data 40

I ANOMALOUS THERMOELECTRIC EFFECT

A. INTRODUCTION

One of the unsolved problems in the study of shock waves in solids is the measurement of temperature behind a shock wave. Some radiation measurements of shocked materials have been and are being made at Los Alamos Scientific Laboratory.[13] For opaque solids this measurement must be made at a free-surface and gives the temperature of material which has been shocked and subsequently released to zero pressure.

It was in attempting thermocouple measurement of the temperature rise across a shock front in a metal that unexpectedly high signals were observed by the laboratories mentioned in the Foreword. To label the signals "unexpectedly high" requires some elaboration—just what should we expect from a thermocouple under these conditions?

In the first place there are the technique problems associated with the short rise time, brief duration and high stress of the shock, the finite size of specimens, etc., which are the subject of the major portion of this section of the report. But beyond this there are more fundamental questions:

1. Is thermal equilibrium attained as assumed in the calculation?
2. How accurate are the theoretically determined temperatures?
3. What is the effect of pressure on thermal emfs?

To be specific, let us consider the case of copper shocked to 390 kb, for which the calculated temperature rise is 280°C.[14] The calculation assumes an adiabatic process in which thermal equilibrium is attained and dissipative phenomena are absent. The adiabatic assumption is reasonable in light of the short rise time (<0.1 μsec) of the shock front. It is generally believed that the time required to attain thermal equilibrium is of the order of λ/c, where λ and c are phonon mean free path and velocity, respectively. Typical values for λ and c are 5×10^{-7} cm and 5×10^{5} cm/sec or $\lambda/c \sim 10^{-12}$ sec—very short compared with times of

measurement. For real explosive assemblies, only quasi-thermal equilibrium is attained because a temperature gradient will be present behind the shock.

The remaining uncertainty in calculated shock temperatures arises from our ignorance of equations of state for solids. The commonly used Grüneisen equation of state, relating thermal (or phonon) pressure to the thermal vibrations of the lattice through a parameter $\gamma(v)$, should be valid at the relatively low pressures and temperatures of the present experiments. The uncertainty of the volume dependence of the Grüneisen parameter γ, however, leads to increasingly uncertain temperatures with increasing shock strengths. For copper at 390 kb, the calculated temperature rise of 280°C is probably accurate to within 20%.

The effect of pressure on thermoelectric powers is difficult to measure. The work of Bundy[15] indicates that a hydrostatic pressure of 72 kb, with a temperature difference of 100°C, produces only a small effect on the thermal emfs of several thermocouples (4% for Cu-constantan).

On the basis of the foregoing comments, it might be concluded that the signal produced by a thermocouple traversed by a not-too-strong shock wave should indeed be predictable if the temperature rise is known, or conversely, should be a reasonable clue as to the actual temperature. That this conclusion may be somewhat naive, or at least premature, is suggested by the realization that, in order to measure the emf produced by a shocked thermocouple, both metals comprising the circuit must contain shocked and zero-pressure regions. That mechanisms exist to produce a potential difference across a shock front in a metal has been realized for some time, but quantitative estimates of magnitude do not yet exist. Also, although we can and do often ignore the fact, shock compression of metals is not strictly hydrostatic. As we move into the new field of electrical properties of shocked solids, it must be kept in mind that the electronic properties may be altered by the anisotropic strain produced by a plane shock wave.

We have, therefore, approached with open minds the problem of thermocouple measurements in shocked solids. The experimental program has been directed toward the determination of whether the "anomalous" effect is an intrinsic property of the system, the measurement of its magnitude, and the study of its properties in order to understand its source.

B. EXPERIMENTAL PROGRAM

Ten shots were fired on this program, two of which produced questionable data apparently because of electronic difficulties. Pertinent shot details are given in Table I. Figure 1 shows the basic electronic circuitry used in all shots (except where cathode followers were omitted—Table I) and Fig. 2 shows the experimental arrangement for the first two shots. These and subsequent shots used 1-inch × 5-inch-diameter explosive pads initiated by 4-inch, P-40 plane-wave lenses. The lenses in turn were initiated by a strand of primacord 24 inches long to allow decay of the electrical noise from the electronic detonator unit. The probes were ½ inch from the HE-specimen interface (except for shots 9145-6), and the specimen was at least 3 inches in diameter and hence effectively infinite in lateral extent. The specimen blocks were fabricated from either OFHC copper or 1100 F aluminum.

For Shots 8682 and 8683, the probes, insulated by Pliobond impregnated paper, were 20-mil wire placed in 25-mil holes. The holes were made with flat-ended drills, and the ends of the wire probes were ground flat. Shot 8682 had one probe of constantan and was intended to determine the amplitude of signal to be expected as well as check out the electronics. Shot 8683 had probes of constantan, iron, aluminum, and copper. Each probe was connected by a 0.001 μf capacitor to the grid of a cathode follower (input impedance $\sim$2 meg, rise time $\leq$ 20 μsec) mounted directly above the copper specimen block. The cold junction of the thermocouple was the probe-capacitor lead junction.

The observed signals are shown in Figs. 3, 4, and 5. The voltage scale on these oscilloscope traces must be multiplied by -2.22 to compensate for the gain (=0.45) of the cathode followers and the fact that negative signals are obtained because of the need for grounding the specimen block. The observed signals, including this factor, are listed in Table I, as well as the signals expected on the basis of atmospheric pressure thermopowers. There is a discrepancy of an order of magnitude (yet the observed signals are about one-half that expected from Jacquesson's work[3]).

The possibility exists that the temperature was really much higher than believed because of a local heating effect due to trapped air and/or converging shock geometry at the probe boundaries; but the inferred

Table I

THERMOELECTRIC EXPERIMENTS

SHOT NO.	HIGH EXPLOSIVE[a]	SPECIMEN BLOCK	PROBE[b]			ESTIMATE OF SHOCKED STATES[c]						JUNCTION $T = \frac{1}{2}(T_{Refl} + T_{Tran})$	EXPECTED[d] SIGNAL (mv)	MEASURED PEAK SIGNAL (mv)	COMMENTS
						Specimen Block				Probe (Transmitted Wave)					
						Incident Wave		Reflected Wave							
			Material	Diam. (in.)	Insulation	P(kb)	T(°C)	P(kb)	T(°C)	P(kb)	T(°C)				
8682	Comp B-3	OFHC Copper	Constantan	0.020	"Pliobond" Impregnated Paper	390	300	400	310	400	270	290	13.7	133 ± 10	
8683	Comp B-3	OFHC Copper	Constantan	0.020	"Pliobond" Impregnated Paper	390	300	400	310	400	270	290	13.7	133 ± 10	
			Fe	0.020	↓			360	290	360	380	335	?	30 ± 10	Fe transforms to new phase. From low-pressure phase, predict −1.4 mv
			Al	0.020	↓			220	230	220	260	245	0.93	20 ± 10	
			Cu	0.020	↓			None		390	300	300	0	< 5	
8745	Comp B-3	OFHC Copper	Al	1.0	Teflon	390	300	220	230	220	260	245	0.93	--	No measurements - electronic difficulties
8746	Comp B-3	OFHC Copper	Al	1/16, 1/8, 1/4, 1/2	Teflon	390	300	220	230	220	260	245	0.93	--	No measurements - electronic difficulties
8889	Comp B-3	OFHC Copper	Constantan[e]	1/8	Unconfined	390	300	400	310	400	270	290	15.4	70 ± 5	
			↓	1/4	↓									70 ± 5	
				1/2										84 ± 5	
				3/4										80 ± 3	
8890	Comp B-3	1100 F Aluminum	Constantan[e]	1/8	Unconfined	240	290	380	350	380	230	290	14.0	82 ± 5	
			↓	1/4	↓									88 ± 5	
				1/2										100 ± 5	
				3/4										100 ± 13	
9145	Baratol	OFHC Copper	Constantan[e]	1/2	Teflon	160	95	165	100	165	65	82	3.1	90 ± 4	
9146	Comp B-3	OFHC Copper	Constantan[e]	1/2	Teflon	360	285	370	295	370	240	265	13.7	72 ± 4	
9332	Baratol	OFHC Copper	Constantan[e]	1/2	Teflon	170	100	175	105	175	70	88	3.4	23 ± 4	Diffusion welded junction (probably incomplete)
			↓	1/2	↓									34 ± 4	No cathode follower
9333	Comp B-3	OFHC Copper	Constantan[e]	1/2	Teflon	390	300	400	310	400	270	290	15.4	42 ± 4	Diffusion welded junction (probably incomplete)
			↓	1/2	↓									73 ± 4	No cathode follower

[a] One inch thick, initiated by P-40 4-inch plane-wave lens.

[b] Probe spaced 1/2 inch from HE-specimen interface except for shots 9145-6 for which distance was 3/4 inch.

[c] Hugoniot data for Cu and Al from Ref. 14; for Fe from Ref. 19. Hugoniot for constantan assumed to be average (in pressure-particle velocity plane) of Hugoniots for Cu and Ni. Temperatures for reflected waves are rough estimates.

[d] Signal calculated on basis of zero-pressure thermopowers.

[e] Probe from constantan (55% OFHC Cu, 45% electrolytic Ni) cast by Metallurgy Section of SRI. Measured emf against Cu for $\Delta T = 100^{\circ}C$ was 4.8 mv, compared with handbook value of 4.28. "Expected signal" includes approximate correction in ratio 4.8/4.28.

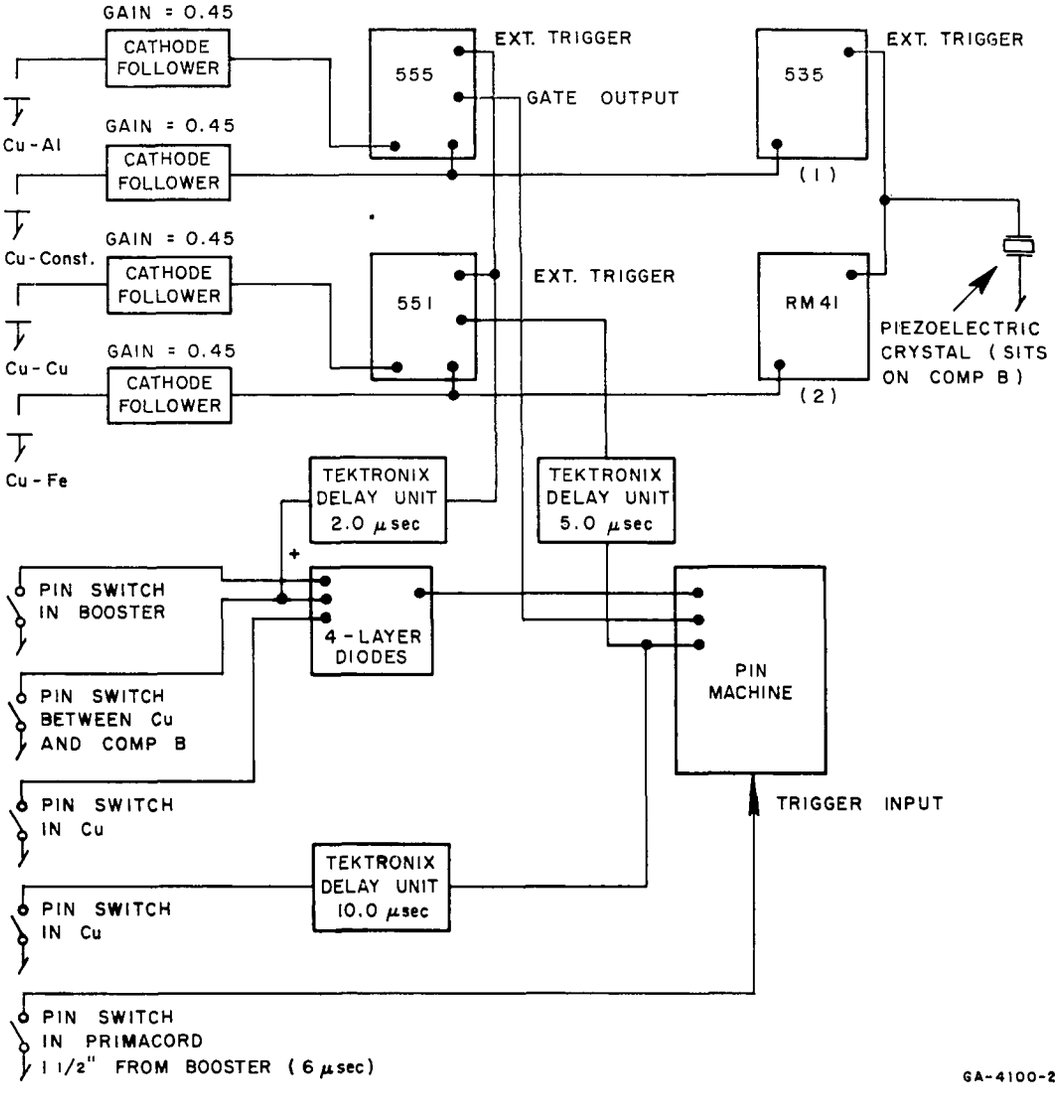

FIG. 1 BLOCK DIAGRAM OF RECORDING CIRCUITS USED FOR SHOT 8683
For Shot 8682 Only One Cathode Follower Was Used and Its Output Was Applied to All Oscilloscopes

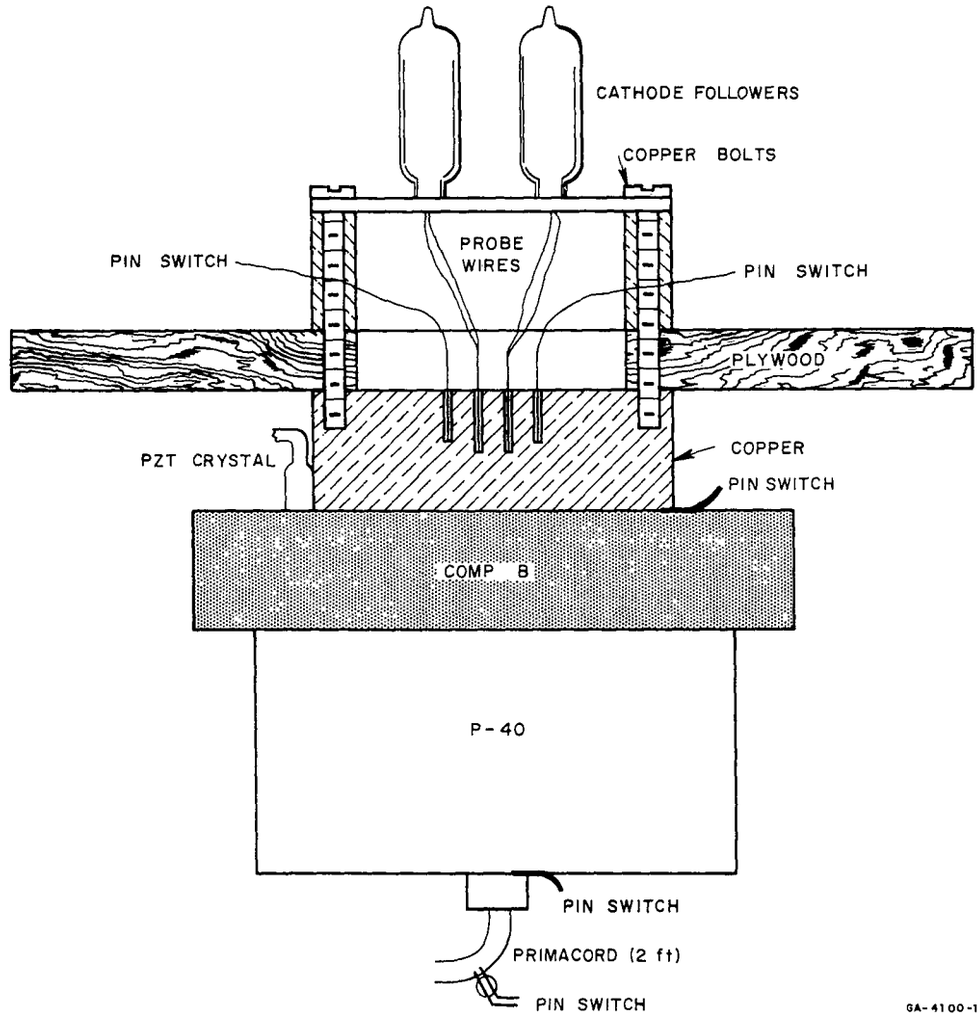

FIG. 2 SCHEMATIC DIAGRAM OF SHOT 8683
In Shot 8682 Only One Constantan Probe
and One Cathode Follower Were Used

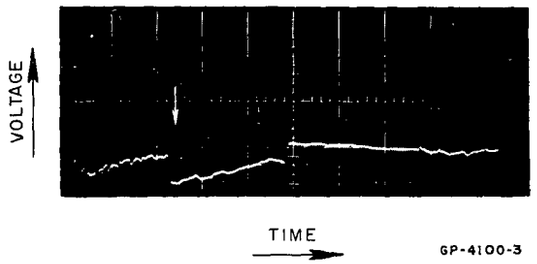

FIG. 3 SIGNAL FROM CU-CONSTANTAN JUNCTION IN SHOT 8682
Record is from RM41 with Sensitivity of 0.1 volt/cm and Sweep Speed of 1 μsec/cm. Calculated Arrival Time of Shock Front at Cu-Constantan Junction is Indicated by Arrow

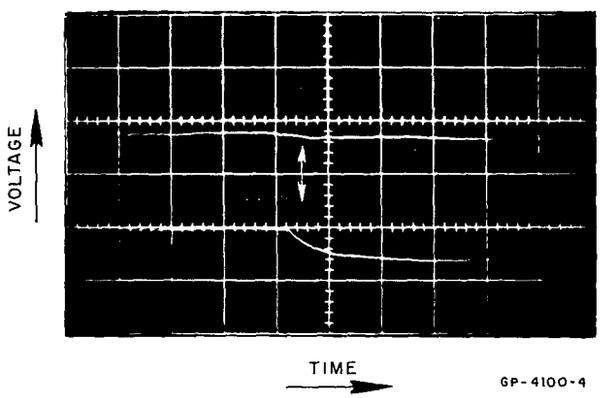

FIG. 4 SIGNALS FROM CU-AL JUNCTION (Upper Trace) AND FROM CU-CONSTANTAN JUNCTION (Lower Trace) IN SHOT 8683
Record is from 555 with Sensitivity of 0.1 v/cm and Sweep Speed of 0.1 μsec/cm (Both Traces). Calculated Arrival Time of Shock Front at Junctions is Indicated by Arrow

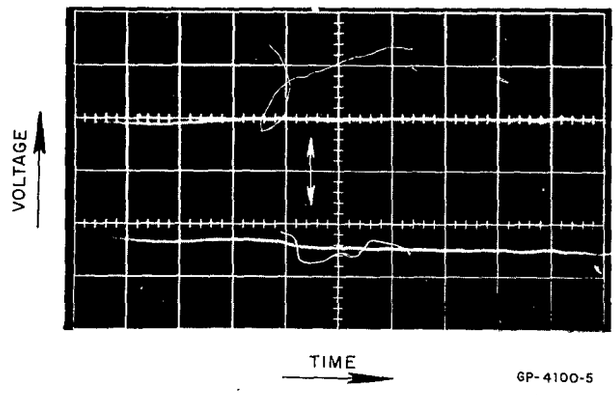

FIG. 5 SIGNAL FROM CU-CU JUNCTION (Upper trace) AND FROM CU-FE JUNCTION (Lower trace) IN SHOT 8683. The Record is from 551 with Sensitivity of 0.1 v/cm and Sweep Speed of 0.1 μsec/cm (Both traces). Calculated Arrival Time of Shock Front at Junctions is Indicated by Arrow

temperatures exceed the melting points of the metals.* It is interesting to note that the relative magnitudes of the signals from the different junctions are consistent with a given temperature increase. The signal from the Cu-Fe junction cannot be predicted because the shock strength is well above 130 kb, and hence the iron is in a high-pressure phase,[16] the thermopower of which is unknown.

It should be pointed out that the signals occur within 0.1 μsec of the arrival time of the shock at the probes, which is about the uncertainty in the time calibration of the shot. The long rise time of approximately 0.1 μsec was unexpected.

It seemed of interest to look for a variation of signal with junction area while simplifying probe construction. Constantan of appropriate dimensions was not readily available so aluminum probes of 1/16-, 1/8-, 1/4-, and 1/2-inch diameter were inserted in one copper block and a 1-inch aluminum probe in another. The instrumentation was as in Fig. 1 and probe construction as in Fig. 6. The oscilloscope records obtained from these shots are not understood. The single probe of Shot 8745 produced no apparent signal and the records from the 551 and 555 oscilloscopes do not

* This assumes reasonable extrapolations of fusion data taken at lower pressures and is, of course, based on zero-pressure thermopowers.

correspond. For Shot 8746 there are apparent signals of about 27 mv amplitude and very slow rise time, but they are about 0.4 μsec late (551 and 555 oscilloscopes disagree somewhat as to timing).

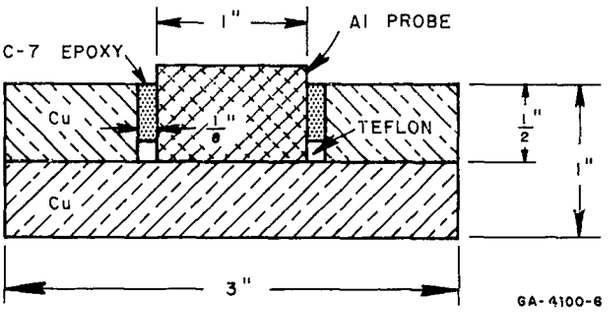

FIG. 6 PROBE ARRANGEMENT FOR SHOTS 8745 AND 8746. Cathode Followers Mounted as in Fig. 2. Plywood Guard Ring in Fig. 2 Replaced by Copper Shield Enclosing Cathode Followers

No data have been used from these shots. A small air gap is believed to have existed between the Teflon ring used to center the probe and the bottom copper plate. This could have provided a conducting ring which possibly shorted out the anticipated signals.

The experimental arrangement for Shots 8889-90, shown in Fig. 7, was designed to look for a possible dependence of signal amplitude on electrode area. The electrodes were constantan* of ¾-, ½-, ¼-, and ⅛-inch diameter. Electrode and specimen surfaces were lapped. Only the initial rise of the signal should be representative of the shocked state for an unconfined probe because a rarefaction wave from the periphery will immediately begin to reduce the stress and temperature. The peak amplitudes are given in Table I and the signals for ¼- and ½-inch probes in Fig. 8.

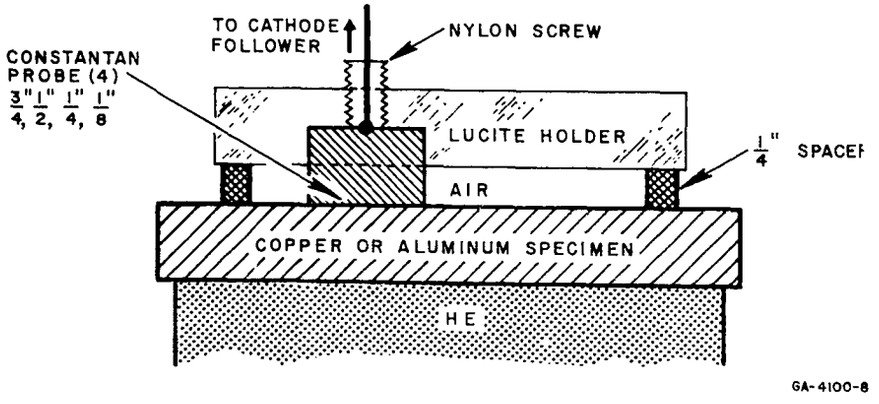

FIG. 7 EXPERIMENTAL ARRANGEMENT FOR SHOTS 8889 AND 8890

* Cut from a 1-inch-diameter bar cast by the Metallurgy Section of SRI (55% OFHC copper and 45% electrolytic nickel).

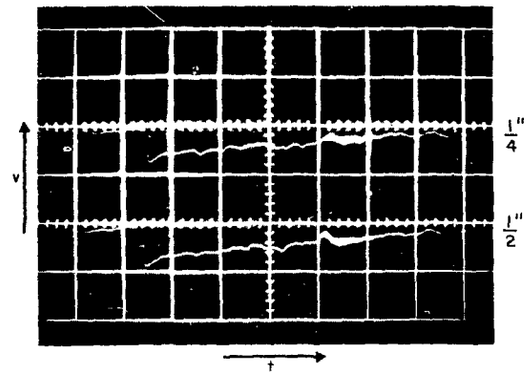

(a) ALUMINUM-CONSTANTAN (SHOT NO. 8890)

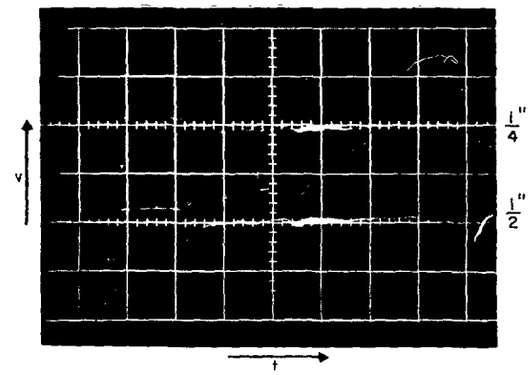

(b) COPPER-CONSTANTAN (SHOT NO. 8889)

GP-4100-9

FIG. 8 SIGNALS OBSERVED IN SHOT GEOMETRY OF FIG. 7. For All Traces, Voltage and Sweep Sensitivities are 0.05 v cm and 0.2 μsec cm

There is a suggestion of a small-diameter effect for both metals. The highest copper-constantan signal was only 84 mv compared to 133 mv observed in the earliest shots (8682 and 8683) using 20-mil insulated wire probes. The signal decayed more rapidly in these shots, but this was expected. It may be that an equilibrium value was not reached, as perhaps indicated by the fact that the rise time was shorter than the 0.1 μsec observed in Shot 8683 and the initial decay required about 0.1 μsec.

Perhaps the most interesting result is that the signals for copper-constantan and aluminum-constantan are in the same ratio as the "expected" thermal emf's. This again suggests that the signals are indeed of thermoelectric origin.

The shot configuration was changed once again for Shots 9145-6 (Fig. 9) in an attempt to eliminate edge effects, *i.e.*, we returned to the configuration of Shots 8682-3 but used a construction which would avoid the uncertain boundary conditions associated with embedding wire probes in small diameter holes. The pressure and temperature were varied by using Baratol high explosive for 9145 and Comp B for 9146.

The signals are reproduced in Fig. 10. They are very similar in shape to those observed earlier until the shock has traversed the constantan probe and reached the copper connecting wire, at which time the signal changes sign. The disturbing feature is that the low-pressure shot produced a slightly larger signal than the high-pressure shot, in contrast to results of other workers.[3] The observed signals are compared with estimated temperatures and pressures in Table I.

The signals from Shots 8682-3 using the wire probes did not exhibit an initial spike as did the later shots. The insulation on these wires was about 1-mil thick and may have progressively shorted as the shock moved along the probe; this may, in some manner not yet understood, account for the absence of a spike. The similarity of the spike in the most recent shots with that observed in earlier ones suggests that the relief wave from the periphery of the probe had little influence on the previous shots. The spike may be a reproduction of the shock profile modified by the pressure and temperature sensitivity of the thermal emf; or it may be due to a nonequilibrium phenomenon—either an intrinsic property of the shock loading of an ideal junction; or a property of the nonideality of the junction. The last possibility suggested modifications in junction construction, such as forcing the metals together to cause plastic flow and hence greater contact area, or diffusion welding the junction.

The final pair of shots (9332-3) used the configuration of Fig. 9 and were intended:

1. to repeat the previous pair of shots to determine the reproducibility of the dependence of signal amplitude on shock strength,
2. to determine the effect of omitting the cathode follower, and
3. to determine the effect of diffusion welding the junctions.

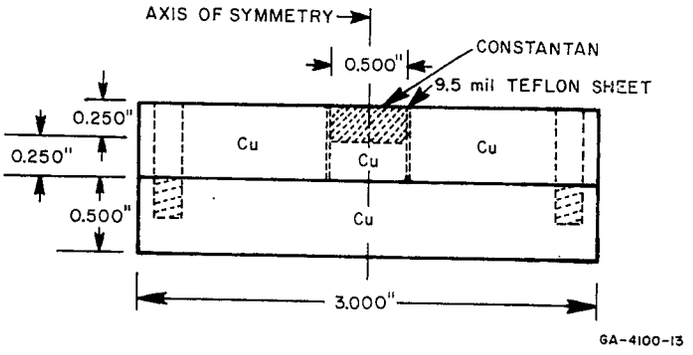

FIG. 9 ASSEMBLY FOR SHOTS 9145 AND 9146

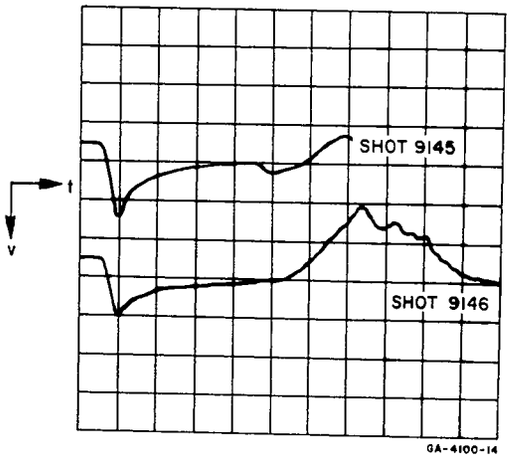

FIG. 10 SIGNALS FROM SHOTS 9145 (Upper) AND 9146 (Lower) Sensitivities are 0.02 v/cm and 0.2 μsec/cm. (Amplitudes must be corrected for gain of cathode follower.)

Each shot was designed to contain two diffusion welded probes—one feeding into the usual cathode follower, and one feeding directly to the oscilloscopes through a terminated 91-ohm cable. During shot assembly, however, two junctions broke apart and it was obvious that diffusion had occurred significantly over only about 50% of the junction area. All traces of diffusion were removed by lapping and butt joints were formed as for earlier shots. Presumably the remaining two junctions were also only partially welded.

This time the weaker shock produced the weaker signal. A comparison of all the signals from shots having the configuration of Fig. 9 is made in Fig. 11. Also included is Shot 8889 in which a ¾-inch constantan probe with no confinement was butted against a copper block.

The Baratol shots exhibit a large variation; in particular, there was no known feature of Shot 9145 which would cause us to question its validity relative to the other shots. Nevertheless, the large signal compared with the other Baratol shots is believed spurious and not indicative of the effects of welding the junction or eliminating the cathode follower. The most obvious explanation is that we are seeing the effect of air trapped at the junction—note that the partially welded junction produced the smallest signal.

On the other hand, the Comp B shots were relatively reproducible. The confined and unconfined junctions gave similar signals, the latter seeming to have a faster initial decrease. This indicates that the relief wave from the periphery is of minor importance or else the attempt at confinement was ineffective. Omitting the cathode follower sharpened the initial rise and fall of the signal and it appears that a cathode follower is unnecessary. The effect of the partial weld was to remove the initial spike (not true for the Baratol shot). It should be said that the reproductions of traces in Fig. 11 are not all equally precise because some of the oscilloscope traces were noisier than others. We have not been completely successful at keeping the noise level consistently low.

C. DISCUSSION

It should be obvious from the preceding description that the few experiments performed to date yield no definite conclusions regarding the thermoelectric behavior of shocked metals.

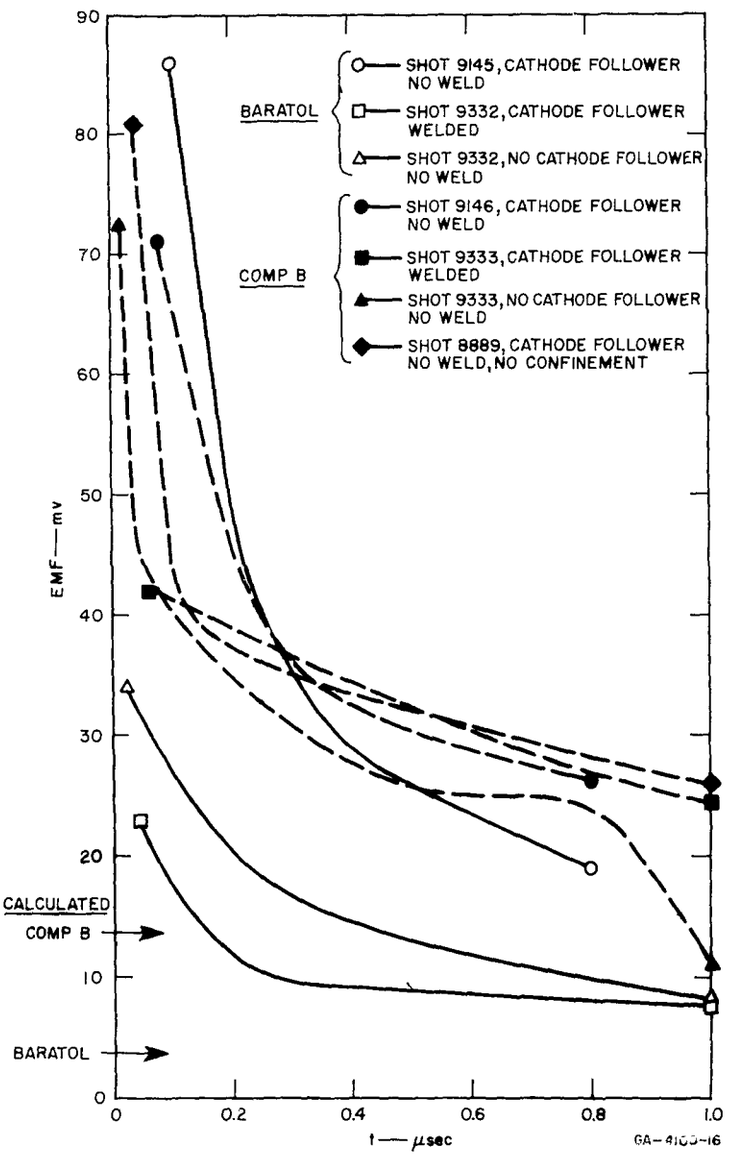

FIG. 11 SIGNALS FROM THERMOELECTRIC SHOTS

That the signals observed from certain combinations of metals (elements and alloys) are higher than expected from calculated equilibrium temperature and zero-pressure thermopowers is well established. It has not been established, so far as we know, that this effect exists for more than a few metals. In the present study, constantan was used as one side of most junctions because the resulting signals were relatively large and hence most conveniently measured. The price paid for this convenience was a less well-known electronic structure and uncertainties in calculated shock pressures and temperatures because of the lack of a Hugoniot for constantan. Additionally, we can no more than suggest that anomalous signals are observed for Cu-Al and Cu-Fe junctions because only one shot was fired in each case. The lack of success in the Cu-Al shots is believed due to electronic difficulties, but it is possible that the signals were *not* anomalously large and went unobserved. Other published work adds little information on this point—Jacquesson[3] used copper-constantan and iron-constantan junctions and Ilyukhin and Kologrivov[4] studied Cu-Ni junctions. Hence only a very limited number of combinations have been studied, and each involves one or more of the transition metals Ni and Fe, Cu, and constantan.

The experiments suggest that the signals are thermoelectric in origin, in that combinations of metals giving large thermal emfs at zero pressure also give large signals when shocked. This is to say that the same electronic properties of the metals are involved in the two cases. On the other hand, the signals were more nearly proportional to shock pressures than to calculated shock temperatures, as was also observed by Jacquesson[3] and (less clearly) by Ilyukhin and Kologrivov.[4] That this is simply a pressure effect on thermopowers is not borne out by the static experiments of Bundy,[15] but further static work needs to be done. A gross extrapolation of his data predicts a change in the thermal emf of -2.5 mv at the maximum pressure and temperature (calculated) of the present experiments.

We must then tentatively conclude that the observed effect is due to temperatures much higher than calculated and/or some phenomena characteristic of shocked solids.

A gross extrapolation of zero-pressure Cu-constantan data indicates temperatures of about 1000°C for the maximum signals of Fig. 11. If the temperature is really much higher than calculated, it might be due to trapped air, or to local heating due to excessive plastic deformation at

the interface. In either case, we would expect the temperature to be reduced by diffusion welding the junction, and, indeed, Fig. 11 indicates that the peak signal was reduced by (imperfect) diffusion welding.

Another possibility is that to attain thermal equilibrium requires much longer than the 10^{-12} sec usually assumed and such equilibrium was never attained in these shots. An upper limit to the nonequilibrium temperature might be estimated by assuming that all the internal energy initially goes into vibrational motion of the lattice, *i.e.*,

$$(\Delta T)_{max} = \frac{\Delta E}{C_v} = \frac{1}{2}\frac{PV_0}{C_v}\left(1 - \frac{V}{V_0}\right) \simeq 1200°C$$

for copper at 400 kb. This is in the neighborhood of the 1000°C roughly estimated above.

A solid subjected to a plane shock wave undergoes one-dimensional strain. Hence the stress in the shock direction will exceed the lateral stress by an amount dependent on the yield strength of the solid. The resulting distortion of the crystal lattice, and hence the Brillouin zones, may be significant because the thermopower of a metal can be expressed in terms of the rate of change of the area of the Fermi surface with energy (evaluated at the Fermi energy).[17]

Another difference between the shock case and the static experiment of Bundy[15] is that in the latter the temperature gradient is at constant pressure and the pressure gradient at constant temperature, whereas in the former the two gradients occur simultaneously.

It has been suggested[18] that the effect may be purely dynamic in nature, caused by preferential scattering of electrons at the shock front. A signal so produced should be highly area sensitive, however, contrary to our results.

We believe that this investigation should be continued and suggest that future work should include the following:

1. Make a theoretical study of the condition at the junction of two dissimilar metals when subjected to a shock wave.
2. Use a better defined input pulse, *e.g.*, a flying plate.

3. Investigate a number of materials--in particular, those metals whose electronic properties are best understood.

4. Repeat the diffusion welding experiments--carry out welding in high vacuum.

5. Study a welded junction with the interface perpendicular to the shock front rather than parallel to it.

6. Study a compressible material, such as lead, and look for indication of melting.

7. Vary the temperature independently of the pressure by varying the initial temperature.

8. Go to much higher pressures with Cu-constantan.

II ELECTRICAL RESISTIVITY

A. INTRODUCTION

The present investigation has been concerned with obtaining quantitative resistivity data as a function of shock stress for the three alkali halides, NaCl, CsI, and KI. Alder and Christian[5] and Al'tshuler *et al.*[10] have reported dramatic decreases of resistivity in these salts above about 200 kb.

The emphasis of the present study has been primarily experimental, with particular attention focused on the following points.

1. To suppress impurity conduction, only optical quality single crystal* specimen material was used. The specimens were fabricated to carefully controlled dimensions. The use of single crystals offers several other advantages:
   a. exclusion of air which could give rise to spuriously low resistance values;
   b. better calculation of pressure, temperature, and specific volume of the shocked specimen;
   c. the possibility of studying anisotropy in resistivity if produced by one-dimensional shock compression.
2. The position of the shock was monitored by precise electronic timing so that electrical signals could be correlated with the stress state of the specimen.
3. Geometrical arrangements, and electrode and specimen dimensions were varied.
4. To exclude spurious effects produced by electrical conduction via paths other than through the specimen, a variety of insulating materials and mechanical arrangements were tested.

Only preliminary consideration has been given to possible mechanisms which might account for the pronounced drop in resistivity. In pure specimens of alkali halides at atmospheric pressure, conduction is by diffusion of ions by means of lattice vacancies. In spite of the high

*CsI was an exception. See Section II-B-4.

pressures involved in the shock experiments, it is not obvious that this mechanism, operating at the very high temperatures reached by shock compression, can be excluded as a possible explanation of the observed effect. The effect of shock compression on the vacancy concentration is unknown.

On the other hand, Alder[20] has attributed the increase of conductivity of these salts to the onset of electronic conductivity, made possible by a pronounced decrease in the energy gap between valence and conduction bands.

Future work will be directed toward determining the correct mechanism, whereas the object of the present work was to verify the phenomenon and make measurements of it.

Another interesting phenomenon observed in this work is that of charge generation when a shock propagates through an alkali halide crystal. This effect appears similar to that reported by Eichelberger and Hauver[21] for a variety of materials. It may be related to the strain-induced charge generation observed in NaCl in quasi-static experiments[22] where it is attributed to motion of charged edge dislocations.

It should be noted that only a rather narrow range of shock stress has been investigated for CsI and KI, and maximum measurable conductivities are still in the semiconductor range. Interesting and perhaps fundamental data should be obtainable by increasing shock strength and developing techniques to measure higher conductivities.

B. EXPERIMENTAL TECHNIQUES

The experimental problem is the electronic measurement in about 1 μsec of the resistance of a shocked material, the magnitude of which may vary over many orders of magnitude. In the present experiments the circuit described by Al'tshuler *et al.*[10] was used (Fig. 12). A constant voltage source is provided by the 2 μf capacitor which is charged to a nominal 80 volts via a 0.5 meg isolating resistor. Conduction in the specimen causes the 2 μf capacitor to discharge, producing a current in the 91-ohm viewing resistor. When the specimen acts as a short circuit, a voltage V_0, in this case + 80 volts, is observed across the 91-ohm resistor. A specimen resistance of R_x ohms may be related to an observed voltage V_x by

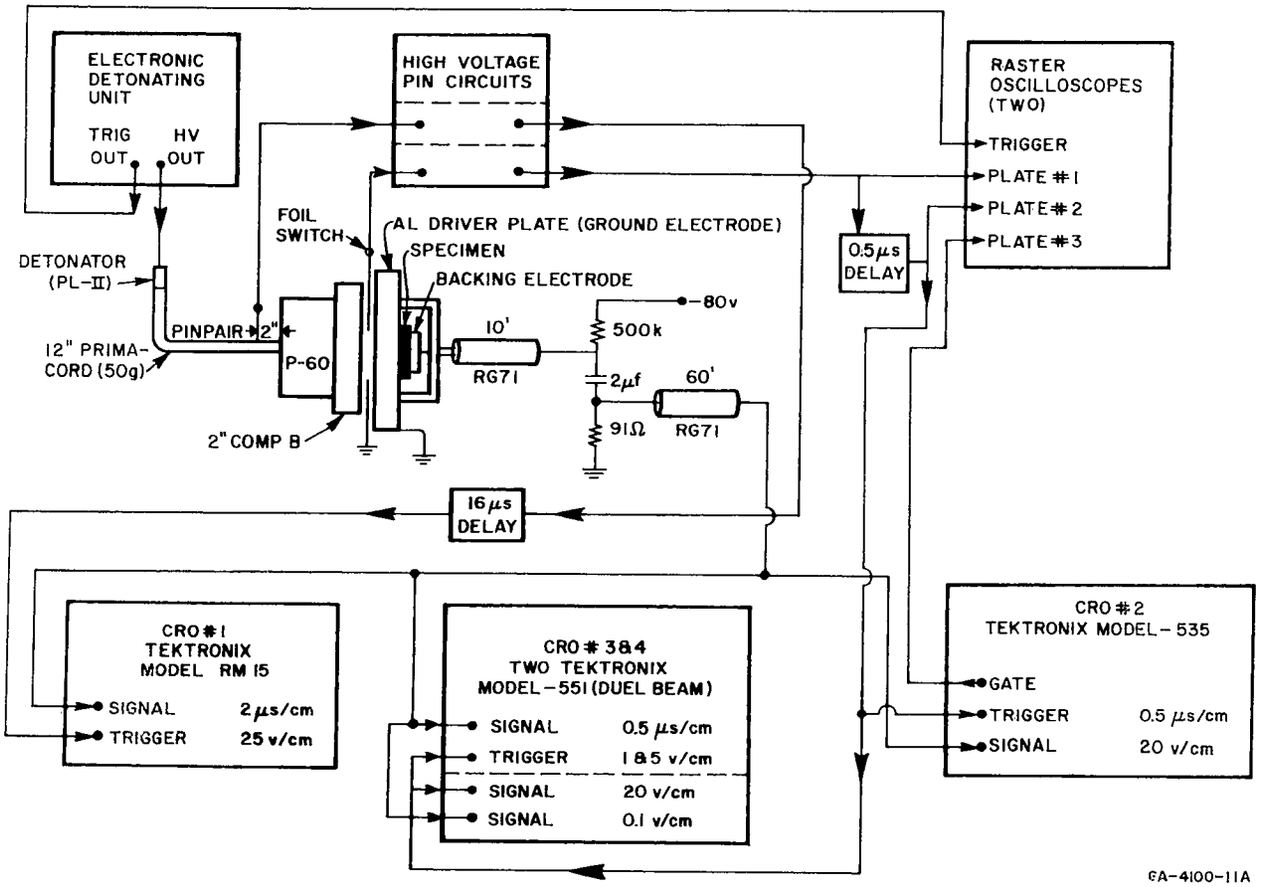

FIG. 12 ELECTRONIC ARRANGEMENT FOR SHOCK RESISTIVITY MEASUREMENTS

$$R_x = R_0[(V_0/V_x) - 1] \quad . \tag{1}$$

In the present arrangement R_0 is 45.5 ohms,* the factor ½ arising because a 91-ohm resistor is used to terminate the 60 feet of RG 71 cable at the oscilloscope. The specimen resistivity ρ is then given by

$$\rho = (AR_0/L)[(V_0/V_x) - 1] \tag{2}$$

where A is the area and L the path length of the current flow.

1. Time Correlation Between Shock Wave Position and Oscilloscope Trace

Because of the short time available in shock-wave resistivity measurements, precise timing of the signal is extremely critical in order that the state of shock stress in the specimen be known in relation to the signals observed on the oscilloscopes.

One way to accomplish this is to trigger the oscilloscope sweeps at a time when the shock front is at a known position in the experimental assembly. The trigger signal used for the fast writing oscilloscopes (CRO 2, 3 and 4, Fig. 12) was produced by a foil switch located at the high-explosive driver-plate interface. The arrival time of a shock front at the driver-plate specimen interface as observed on the oscilloscope sweep may be predicted by subtracting the 0.5 μsec delay (monitored on the raster oscilloscope) from the shock wave transit-time through the driver plate. Additional corrections take into account the signal delay in the oscilloscope as well as the delay produced by possible differences in the length of the trigger and signal cables. The shock front arrival at the specimen-driver plate interface is nearly always accompanied by a small "polarization"† signal (Section II-C-2). The onset of this polarization signal is normally predictable from the above determination to within 0.03 μsec. Synchronization errors of more than 0.05 μsec can usually be attributed to a malfunction of the trigger system, observable on either the slow oscilloscope (CRO No. 1) or the raster oscilloscope. The former, sweeping at 2 μsec/cm, is independently triggered and provides back-up data in case of complete failure of the foil switch triggering system.

---

*Ignores cable resistance.

†This term is used for convenience and does not signify any specific physical mechanism.

2. Longitudinal Configuration

The longitudinal configuration for shock wave resistivity measurements (Fig. 13) is advantageous for reasons other than simplicity. By using a backing electrode of the same shock impedance as the specimen, the measurement can be made on a shock-free specimen. Furthermore, the state in a singly-shocked specimen can be calculated with greater certainty than the state in a multiply-shocked one. By using a relatively large explosive system, the shocked state of the specimen is hopefully maintained long enough for transient electrical effects due to the passage of the shock front to decay, and a "steady state" resistivity signal to be recorded. If the lateral insulating material is also a good impedance match to the specimen (not the case in the present experiments), stress relief via rarefaction waves from lateral boundaries is delayed.

Generally, in the experiments in which the resistivity of the alkali halide remains high, a so-called polarization signal (Fig. 14, and Section II-C-2) begins and ends at times which, to within experimental accuracy, correspond to the entrance and exit of the shock front from the specimen. These signals also appear for all but one of the insulators tested (Section II-C-3). Polarization signals allow determination of shock wave position independently of the foil switch timing system and provide verification of this system. However, in the experiments in which high conductivity was indicated, a recognizable signal was not always obtained upon exit of the shock from the specimen, *e.g.*, see Fig. 15(a) and 15(b).

In order that the time of shock front exit from the specimen be determined independently, the configuration of Fig. 16 was devised. It was designed to indicate precisely shock arrival at the backing electrode while causing minimum perturbation of a simultaneous resistance measurement. The light pipe-photomultiplier system detects a flash of light produced in the trapped air by the shock front arrival at the specimen-electrode interface.* The image of the frosted tip of the light pipe is focused on the face of an RCA No. 6349 photomultiplier tube. The output, delayed less than 0.01 μsec in the tube, is displayed on one of the Type 551 oscilloscopes shown in Fig. 12 along with the conduction signal.

*The gold film evaporated on the specimen acts to shield the light pipe from light generated within the specimen.

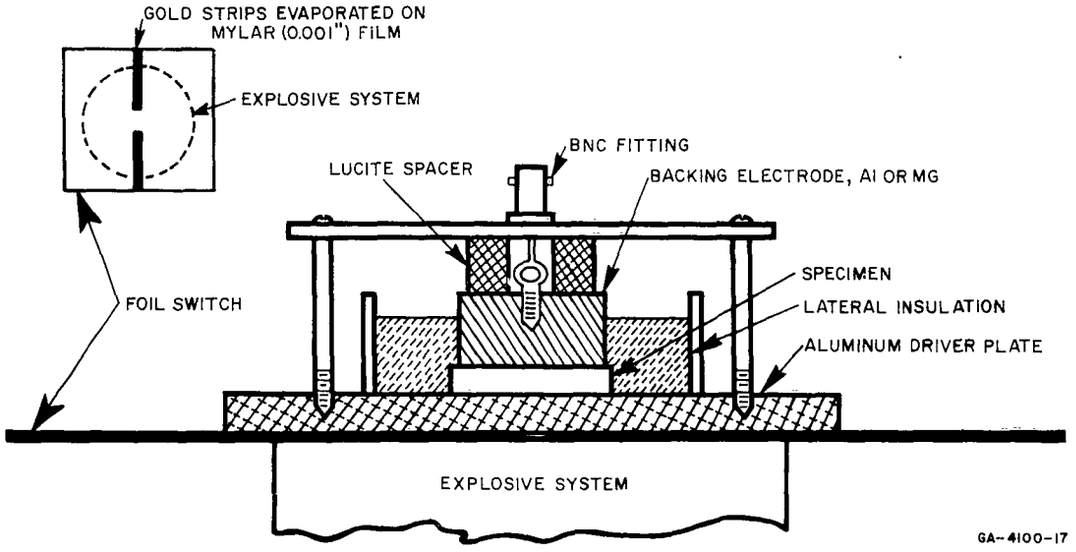

FIG. 13 LONGITUDINAL CONFIGURATION – ELECTRICAL RESISTIVITY MEASUREMENT IN SHOCK-PROPAGATION DIRECTION

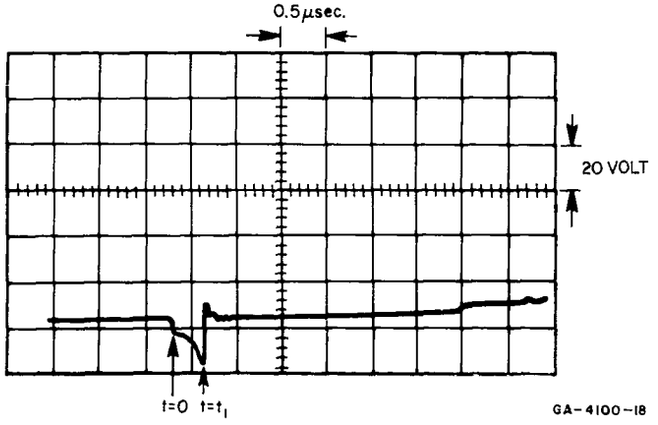

FIG. 14 POLARIZATION SIGNAL FOR NaCl AT 231 kb SHOT 9483

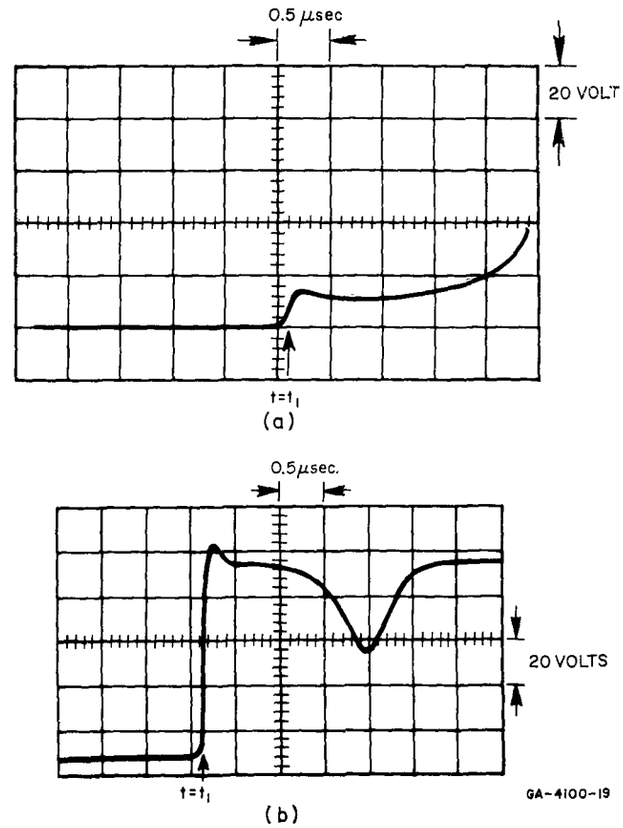

FIG. 15 (a) CONDUCTION SIGNAL FOR KI AT 181 kb (beginning of polarization not discernible at this signal level) – SHOT 9505
(b) POLARIZATION, FOLLOWED BY CONDUCTION SIGNAL (at t = ti) FOR CsI AT 274 kb – SHOT 9489

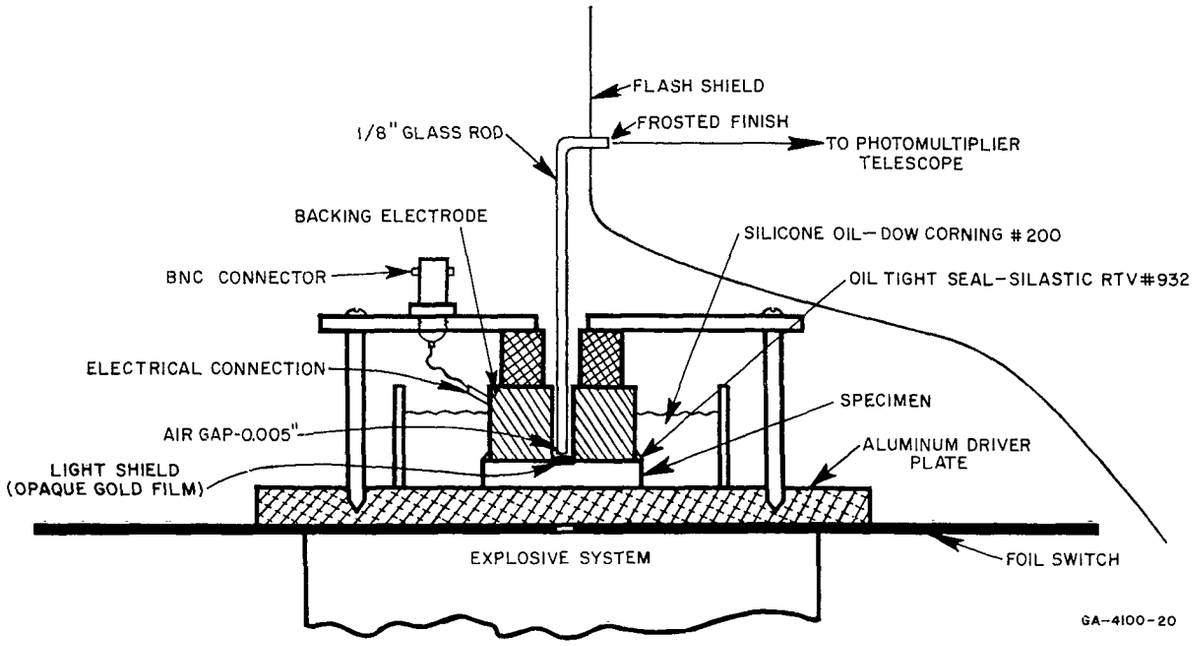

FIG. 16 LONGITUDINAL CONFIGURATION – SHOCK RESISTIVITY MEASUREMENT WITH PHOTOELECTRONIC DETECTION OF SHOCK ARRIVAL AT SPECIMEN-BACKING ELECTRODE INTERFACE

One of the major experimental problems is to eliminate all possible sources of electrical conductivity other than the specimen. Early in this work it was shown that when NaCl was fired in longitudinal geometry at the highest shock strength employed in this study, with only air at atmospheric pressure as a surrounding medium, little or no spurious conduction resulted (Shot 9374, Table II). Nevertheless, even a small signal due to the air will raise the effective noise level and limit the highest resistivities which can be measured, and hence it is desirable to exclude it.

An attempt to learn something of the behavior of the periphery of the specimen when shocked in air resulted in the framing camera sequence of Fig. 17. The composition of the "cloud" is not known, but it is a possible source of spurious conduction.

Both silicone oil (Dow Corning No. 200) and silicone rubber (Dow Corning RTV 932) are thought to be appropriate materials for use as lateral insulation, the former being preferred because of the greater possibility of completely excluding air. The resistivity of both is high (Section II-C-3 and Table IV).

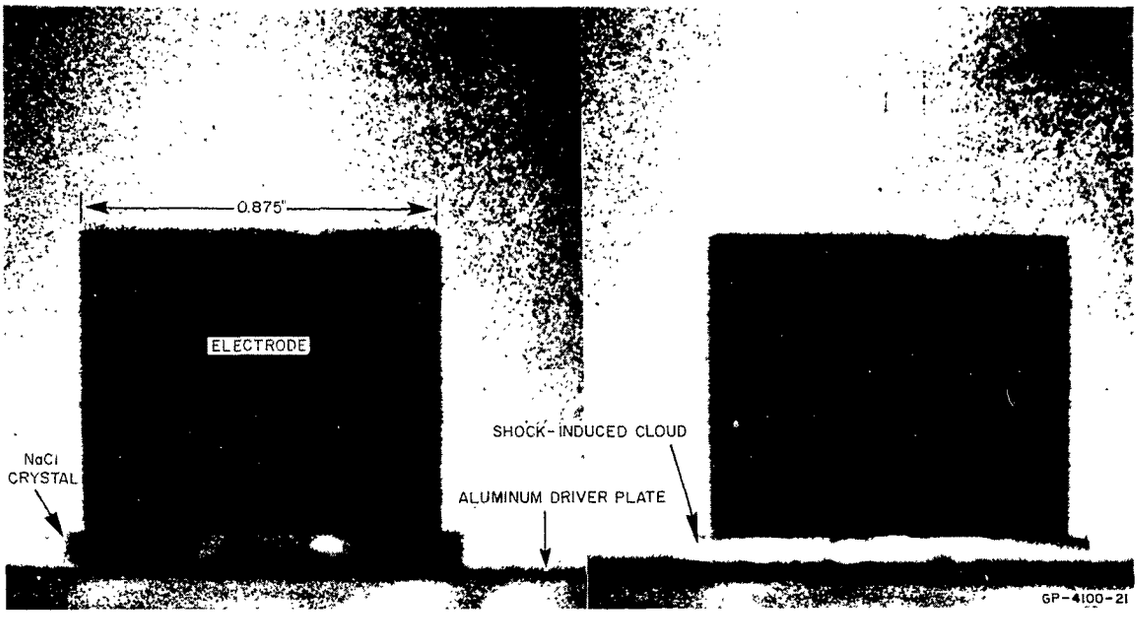

FIG. 17 FRAMING CAMERA SEQUENCE SHOWING SHOCK IN ALUMINUM DRIVER PLATE IMPINGING ON NaCl CRYSTAL SURROUNDED BY AIR – Mock-Up Longitudinal Resistivity Experiment at Specimen Pressure of 231 kb. (Left) Assembly Prior to Shock Arrival at Aluminum Surface. (Right) 0.67 μsec Later – Shock-Front is Approximately at NaCl-Electrode Interface. (Effective exposure time 0.22 μsec/frame; Ektachrome Film, with front lighting by explosive argon source.)

3. Transverse Configuration

Measurement of the electrical conductivity transverse to the direction of shock propagation is desirable because:

a. The results of longitudinal geometry experiments may be in error due to polarization effects persisting after shock transit. This effect can be studied in a passive experiment only if it is not influenced by an applied electric field.

b. The resistivity may be anisotropic with respect to the shock propagation vector.*

If proper nonconducting backing materials are utilized, high shock-stress states in a specimen can be maintained for times comparable to those in longitudinal experiments. The specimen may be subjected to shock stress of a constant or changing intensity by varying the shock impedances of the driver plate and backing block as in the longitudinal experiments.

* It also is possible for the defect structure of the crystal to be anisotropic in the transverse plane, thus providing a possible source of spurious signals (see Ref. 22).

In the present experimental arrangement (Fig. 18) the metal electrodes were chosen to match closely the specimen in shock impedance; therefore they can be assumed to move with the specimen. The driver plate and lateral insulating blocks were made of Hi-D glass, a lead oxide glass found by Keough[23] to be nonconducting under high shock stress. The backing block was made of Arkansas novaculite, a natural polycrystalline quartz material with shock impedance very close to that of CsI[32] (Fig. 19). The experiments using KI and CsI were assembled using epoxy to hold the different blocks together rigidly. A fluid retaining ring of polyethylene was cemented into place on the Hi-D driver plate. The assembly was then placed in a specially designed vacuum chamber, evacuated to 25 microns, and silicone oil was introduced onto the floor of the well formed by the polyethylene ring. After the well was filled, an oil stain appeared on the upper surface where the lateral retaining blocks and the novaculite backing block were in close contact. This was taken to indicate that the oil had traveled along the internal cracks within the assembly and had displaced any remaining air.

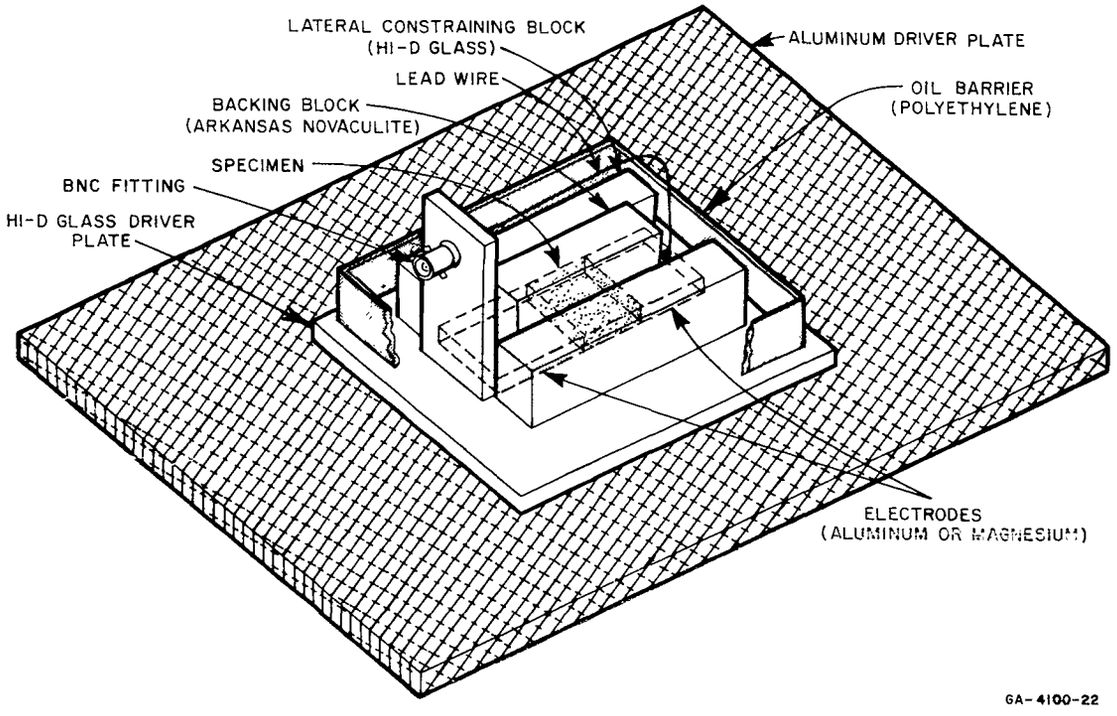

FIG. 18 TRANSVERSE CONFIGURATION – RESISTIVITY MEASUREMENT PERPENDICULAR TO DIRECTION OF SHOCK PROPAGATION

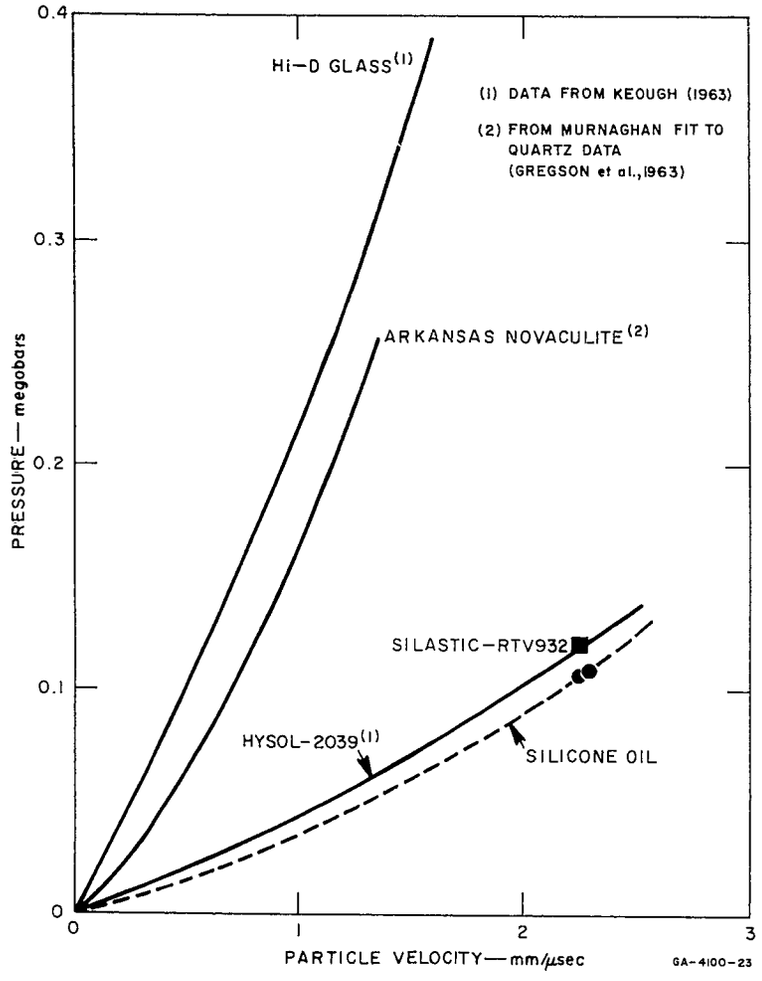

FIG. 19 PRESSURE vs. PARTICLE VELOCITY FOR VARIOUS INSULATORS – Experimental Points are from Shock Velocities Deduced from Polarization Signals

If, as in the case of KI in the present experiment, the shock impedance of the backing block is not closely matched to the specimen, the resistivity appropriate to the state behind the incident shock and to later reflected states must be obtained from the voltage-time relation observed on the oscilloscope. The appropriate analysis is the subject of Appendix A.

4. Specimen Preparation

The specimens of NaCl, KI, and CsI were prepared from optical grade crystals obtained from the Harshaw Chemical Co., Cleveland, Ohio. The NaCl specimens were single crystals. The KI specimens were poor

single crystals in that they contained domains of slight misorientation (±1° according to Harshaw); they were easily cleavable. The CsI specimens were represented as probably being single crystals, with the possibility that they might consist of up to three domains. However, a recent X-ray examination of one specimen, to determine its orientation, disclosed that it was polycrystalline with apparently random orientation of grains. Subsequent microscopic examination of several crystals, after etching with water, revealed boundaries of grains several mm in size. The X-ray examination indicates that these grains may contain sub-domains. Because the specimens were not individually examined prior to firing, we must conclude the CsI specimens were nominally polycrystalline in random orientation.

The KI and NaCl were cleaved to the desired thickness, which for the present experiments varied from 2 to 5 mm. Surface irregularities produced by cleaving were removed by lapping so that the final parallelism was with 0.001 inch. To prepare CsI specimens, the blanks were parted on a lathe to the desired thickness and then lapped. The square shape of the specimens for the transverse experiments was obtained by lapping in a specially made jig. Because KI is particularly hygroscopic it was kept desiccated until shot time.

C. EXPERIMENTAL RESULTS

1. Alkali Halide Resistivity

The results of resistivity measurements on NaCl, KI, and CsI are presented in Tables II and III, and Figs. 20 and 21.* The resistivity of NaCl at 230 kb is still greater than 4×10^5 ohm-cm. The resistivities of CsI and KI, however, decrease dramatically by factors of at least 10^7 and 10^5, respectively, over the shock pressure range studied (perhaps 10^{12} relative to the resistivity at 1 atmosphere and room temperature). The results for NaCl are in significant disagreement with both the Livermore work reported by Alder[20] and the work of Al'tshuler *et al.*[10] The data for CsI and KI are in semiquantitative agreement with the results obtained at Livermore. (Discussion, Section II-D.)

*Where lower limits to the resistivity are indicated in the tables and figures, the signal could not be distinguished from noise. Where upper limits are indicated, the signal could not be distinguished from a short circuit.

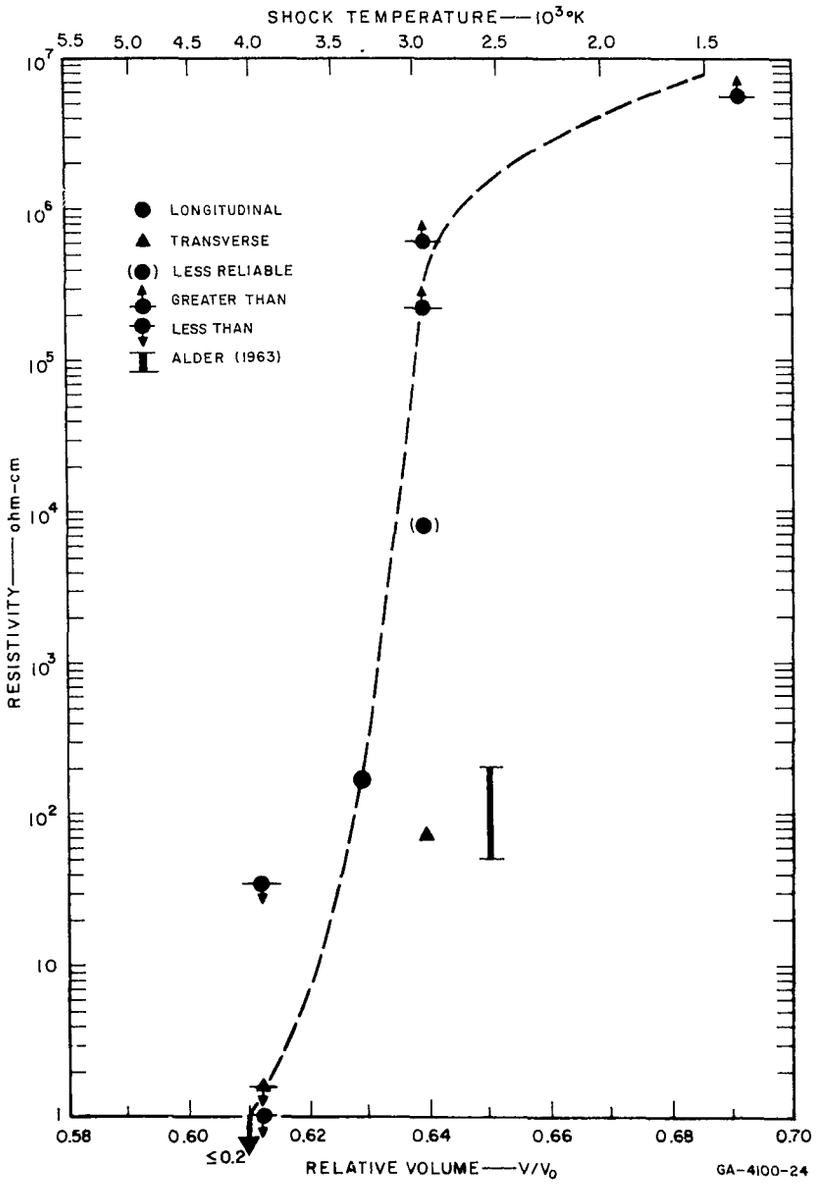

FIG. 20 RESISTIVITY vs. RELATIVE VOLUME AND SHOCK TEMPERATURE FOR CsI

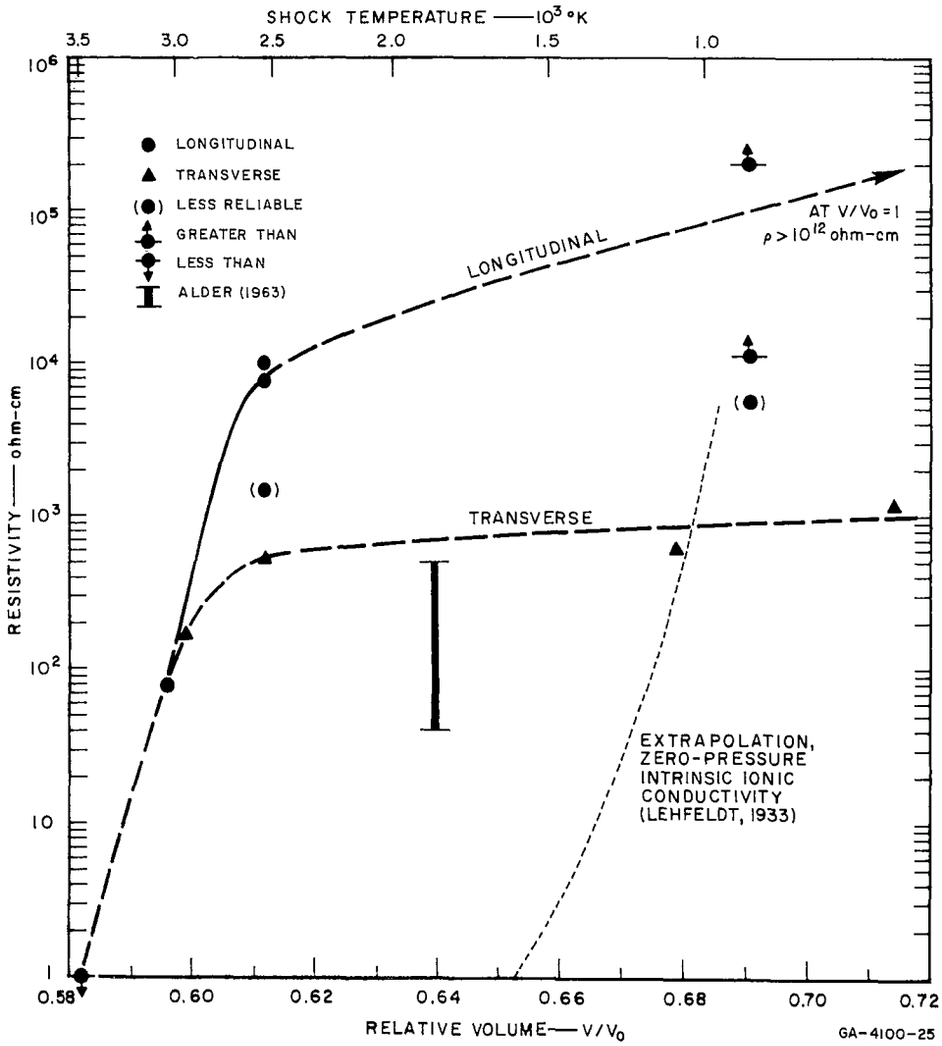

FIG. 21 RESISTIVITY vs. RELATIVE VOLUME AND SHOCK TEMPERATURE FOR KI

Table II

ALKALI HALIDE RESISTIVITY, LONGITUDINAL GEOMETRY[a]

MATERIAL ρ_0 (g/cc)	SPECIMEN THICKNESS[b] (mm)	ELECTRODE DIAMETER (inch)	CONFINING LATERAL INSULATION	HIGH EXPLOSIVE[c]	DRIVER	STATE IN DRIVER[d] σ (kb)	STATE IN SPECIMEN[e] u (mm/μs) σ (kb)	COMPRESSION[e] V/V_0	SHOCK VELOCITY U (mm/μs)	OBSERVED SHOCK VELOCITY U (mm/μs)	RESISTIVITY ρ (ohm-cm)	SHOT NO.
NaCl ρ_0 = 2.16	5.03	0.626	Air	2" Comp B-3	½" Al	294	1.82 231	0.697	6.01	6.14(P)	> 4 x 10^5	9374
	5.01	0.627	CCl_4	2" Comp B-3	½" Al	294	1.82 231	0.697	6.01	6.04(P)	> 6 x 10^5	9375
	2.18	0.875	Silastic RTV 932	2" Comp B-3	½" Al	294	1.82 231	0.697	6.01	6.8(P) 6.1(P)[f]	> 4 x 10^5	9483
	2.69	0.875	Silicone Oil D.C. #200	2" Comp B-3	½" Al	294	1.82 231	0.697	6.01	5.98(P)	> 4 x 10^5	9498
KI ρ_0 = 3.13	3.84	0.938	Teflon	2" Comp B-3	½" Al	294	1.78 233	0.582	4.26	--	(< 1)	9309
	3.29	0.625	Air	2" Comp B-3	½" Al	294	1.78 233	0.582	4.26	4.25(P)[f]	< 1	9376
	3.29	0.626	Air	Bare lens	½" Al	121	0.91 84	0.706	(2.91)	2.57(P)	--	9378
	3.89	0.626	Air	2" TNT	½" Al	237	1.50 181	0.612	3.86	3.89(P)	(1.5 x 10^3)	9383
	3.90	0.626	Air	2" Baratol	½" Al	133	0.98 93	0.691	(3.03)	5.73(P)	(5.7 x 10^3)	9385
	2.41	0.875	Silastic RTV 932	2" Baratol	½" Al	133	0.98 93	0.691	(3.03)	2.77(PM) 2.84(P)	> 2.0 x 10^5	9486
	2.49	0.874	Silastic RTV 932	2" TNT	½" Al	237	1.50 181	0.612	3.86	3.41(PM)	7.7 x 10^3	9487
	2.49	0.875	Silicone Oil D.C. #200	2" Baratol	½" Al	133	0.98 93	0.691	(3.03)	2.62(PM) 2.83(P)	> 1.1 x 10^4	9503
	2.01	0.876	Silicone Oil D.C. #200	2" TNT	½" Al	237	1.50 181	0.612	3.86	3.19(P)	1 x 10^4	9505
	2.46	0.875	Silicone Oil D.C. #200	2" Comp B-3	1" Al	252	1.58 196	0.596	3.96	3.79	77	9507

Table II *Concluded*

MATERIAL ρ_0 (g/cc)	SPECIMEN THICKNESS[b] (mm)	ELECTRODE DIAMETER (inch)	CONFINING LATERAL INSULATION	HIGH EXPLOSIVE[c]	DRIVER	STATE IN DRIVER[d] σ (kb)	STATE IN SPECIMEN[e] u (mm/μs) σ (kb)	COMPRESSION[e] V/V_0	SHOCK VELOCITY U (mm/μs)	OBSERVED SHOCK VELOCITY U (mm/μs)	RESISTIVITY ρ (ohm-cm)	SHOT NO.
CsI ρ_0 = 4.51	5.10	0.938	Teflon	2" Comp B-3	½" Al	294	1.53 274	0.612	3.94	--	(< 1)	9308
	5.03	0.627	Air	2" Comp B-3	½" Al	294	1..53 274	0.612	3.94	4.09(P)[f]	(< 1)	9377
	4.98	0.624	Air	2" Baratol	¼" Al	133	0.86 107	0.691	2.78	3.24(P)	$>4.7 \times 10^6$	9382
	4.96	0.500	Air	2" TNT	½" Al	237	1.31 215	0.639	3.63	--	(8.0×10^3)	9384
	2.67	0.876	Silastic RTV 932	2" Comp B-3	½" Al	294	1.53 274	0.612	3.94	--	≤ 25	9484
	2.67	0.874	Silastic RTV 932	2" TNT	½" Al	237	1..31 215	0.639	3.63	3.81(PM) 4.37(P)	$\geq 6 \times 10^5$	9485
	2.02	0.876	Silicone Oil D.C. #200	2" TNT	½" Al	237	1..31 215	0.639	3.63	2.89(PM) 3.11(P)	$\geq 2.2 \times 10^5$	9499
	2.89	0.875	Silicone Oil D.C. #200	2" Comp B-3	1" Al	252	1.39 231	0.629	3.75	3.83(PM) 4.10(P)	185	9506

[a] Shock propagation and resistivity in [100] direction for NaCl and KI (see Sec. II-B-4).

[b] Diameter = 25 mm.

[c] Initiated by P-40 explosive plane-wave lens (Mason and Hanger, Inc., Amarillo, Texas).

[d] Values used obtained from previous work at this Laboratory.

[e] Calculated from data of Christian (1957).

[f] Determination from another experiment not listed separately.

( ) Less reliable value.

(P) Inferred from time duration of polarization signal.

(PM) Obtained from photomultiplier system.

Table III

ALKALI HALIDE RESISTIVITY, TRANSVERSE GEOMETRY [a]

MATERIAL	SPECIMEN AND ELECTRODE WIDTH (inch)	CONDUCTION PATH (inch)	SPECIMEN AND ELECTRODE THICKNESS (inch)	EXPLOSIVE SYSTEM P40 +	STATE IN ¼ in. GLASS DRIVER [b] u (mm/μs) σ (kb) U (mm/μs)	STATE IN SPECIMEN u_1 (mm/μs) σ_1 (kb) U_1 (mm/μs)	RESISTIVITY-INITIAL SHOCK TRAVERSE (ohm-cm)	STATE AFTER SHOCK REFLECTION u_2 (mm/μs) σ_2 (kb) U_2' (mm/μs)	RESISTIVITY AFTER SHOCK REFLECTION (ohm-cm)	SHOT NO.
CsI	0.695	0.694	0.203	2" TNT ¼" Al	1.12 244 3.53	1.31 215 3.63	71	--	--	9517
	0.695	0.693	0.203	2" Comp B ¼" Al	1.36 316 3.75	1.53 274 3.94	< 1.6	--	--	9518
KI	0.695	0.693	0.157	2" Baratol ¼" Al	0.69 144 3.37	0.98 86 3.43	(1.2 x 10^3)	0.79 114 2.45	0.61 x 10^3	9514
	0.695	0.694	0.156	2" TNT ¼" Al	1.12 244 3.53	1.50 181 3.86	0.52 x 10^3	1.27 236 3.17	0.17 x 10^3	9515

[a] For KI, shock propagation in [100] direction.

[b] Hugoniot data for Hi-D glass, ρ = 6.2 g/cc (Keough, 1963).

The resistivity of CsI seems to change more rapidly with volume (and/or temperature) than that of KI. This is suggested by the curves of Figs. 20 and 21 and also by the following observation. In longitudinal geometry, the time of measurement is limited to about 2 μsec after the shock reaches the backing electrode, because a short circuit generally occurs at this time. During this measurement time the stress and temperature in the specimen are being decreased by the rarefaction wave following the shock wave and, probably more seriously, by rarefactions from lateral surfaces and from that portion of the rear surface not covered by the electrode. In spite of this, the conduction signal for KI remains nearly constant for about 2 μsec [Figs. 15(a) and 22]. For CsI, however, the signal variation with time indicates the initial decrease is followed by a gradually increasing resistance [Fig. 15(b)]. At 274 kb, Shots 9484

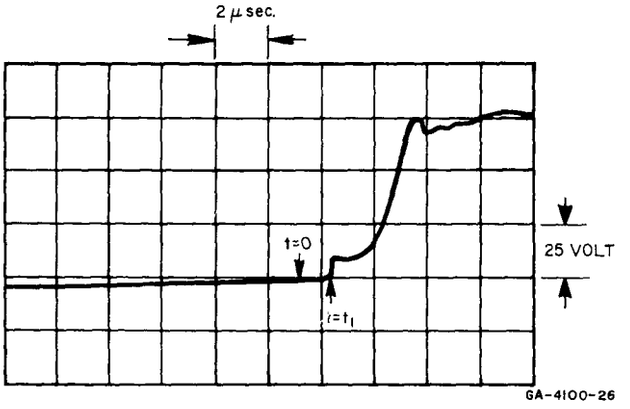

FIG. 22 POLARIZATION SIGNAL FOLLOWED BY STEADY CONDUCTION SIGNAL at $t = t_1$ for KI at 181 kb – LONGITUDINAL GEOMETRY, SHOT 9487

and 9377 indicated apparent resistivities increasing with time from $\leq$ 25 to 400 ohm-cm and from $\leq$ 1 to 160 ohm-cm, respectively. The increase occurred earlier for 9377 (electrode diameter = 0.627 inch) than for 9484 (electrode diameter = 0.876 inch). At 231 kb, Shot 9506 indicated an increase from 77 to 5×10^4 ohm-cm. These observations suggest that the resistivity of CsI is more sensitive to changes of V and/or T than the resistivity of KI, although this is only one possible interpretation.

The results of the transverse geometry experiments (see typical record in Fig. A-1) generally indicated lower resistivities than measured

in the longitudinal geometry, but only the KI data are in serious disagreement with longitudinal geometry data. These results are being viewed with suspicion because the possibility of extra-specimen conduction cannot be rejected at this time. However, the possibility that the conductivity is anisotropic with respect to the direction of shock propagation is being given serious consideration.

Another unexpected result from a transverse geometry shot was the recording of an apparent polarization signal of 2-volt amplitude in a 274 kb CsI shot with zero applied voltage. It began abruptly when the shock entered the specimen and remained steady for 6 μsec.

2. Charge Generation

In all the electrical conduction experiments performed, a signal of presumably electro-mechanical origin was observed upon entrance of the shock front into the specimen. Following the phenomenological description of these signals in dielectrics, the voltage will be termed a polarization signal in the following.

For the materials of high resistivity, the polarization signal appears either as a varying voltage observed as the shock propagates through the specimen [as for NaCl (Fig. 14) and Hysol epoxy] or as a positive or negative voltage "spike" as the shock enters and leaves the specimen (see Fig. 23). The former type has been reported by Eichelberger and Hauver[21] for a large number of dielectrics, including several organic polymers. Allison and Wenzel[24] have formulated a theory relating characteristics of the signal to macroscopic material parameters (assuming zero conductivity of the shocked material). In particular, they found that the initial signal amplitude is determined by the shock induced polarization and is directly proportional to the area and inversely proportional to the thickness of the dielectric. The shape of the signal is determined by the change in electric susceptibility across the shock. This change was determined for polystyrene and was found to correspond to the density change.

The polarization signals for NaCl observed in the present work (Fig. 14) are qualitatively similar to those studied by Allison and Wenzel, but are not proportional to the ratio of specimen area to thickness. This ratio is 3.3 times larger for Shots 9382-3 than for

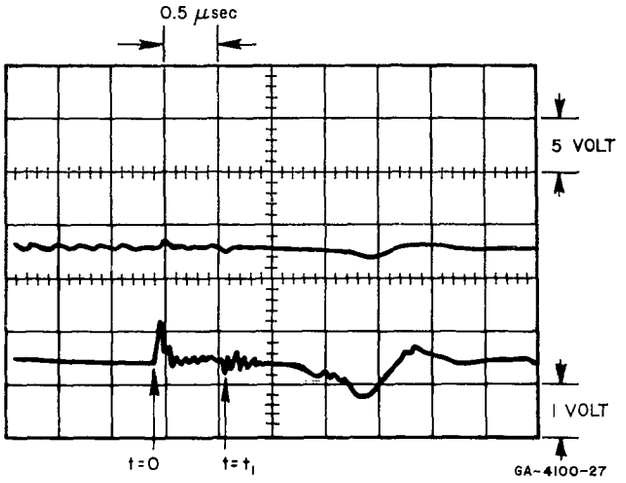

FIG. 23 POLARIZATION SIGNAL (Indicated by Characteristic Ringing) CORRESPONDING TO ENTRANCE AND EXIT OF SHOCK FRONT IN SILICONE OIL AT 106 kb. Signal at $t > t_1$ Believed Not Due to Conduction – SHOT 9504

Shots 9374-5, but the former gave –6.8 and –7.0 volts compared with –4.5 and –3.5 for the latter, a ratio of less than 2.

The decrease in magnitude and the surprising change in sign of the polarization signal observed for CsI as the shock strength was increased are illustrated in Fig. 24, 25, and 26, corresponding to

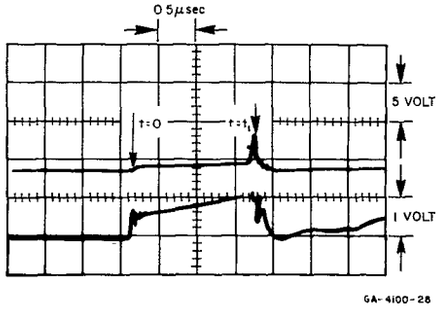

FIG. 24 POLARIZATION SIGNAL FOR CsI AT 107 kb. Noise after Polarization Signal Determines Upper Limit of Reported Resistivity – SHOT 9382

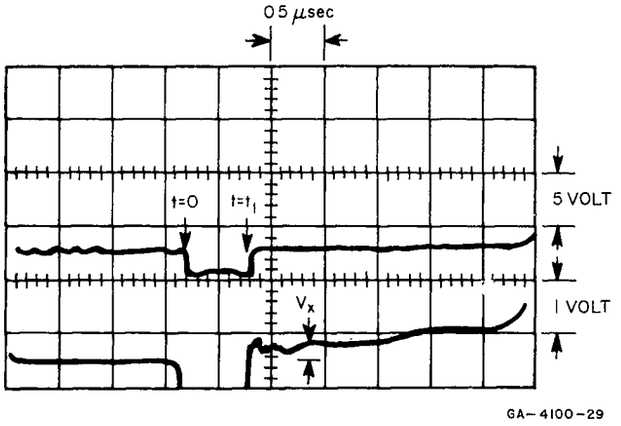

FIG. 25 POLARIZATION SIGNAL AND SMALL CONDUCTION SIGNAL FOR CsI AT 215 kb – SHOT 9499

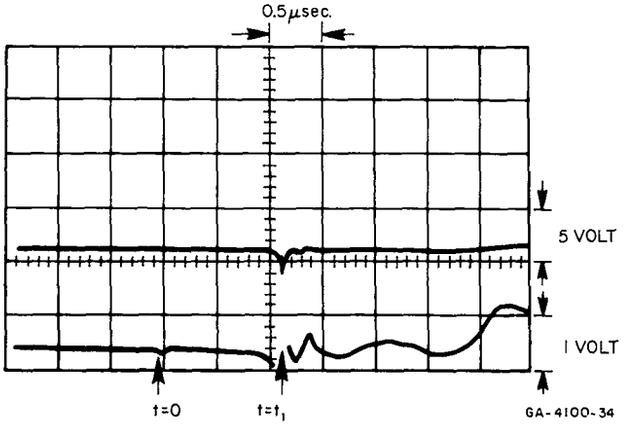

FIG. 26 POLARIZATION SIGNAL IN PASSIVE EXPERIMENT WITH CsI AT 274 kb. Noise at $t > t_1$ Apparently Generated by Specimen – SHOT 9380

107, 215, and 274 kb, respectively. The 274 kb shot was passive (*i.e.*, no applied field). Presumably the onset of conduction accounts for the reduction in magnitude of the polarization signal.

Above 230 kb in CsI [Fig. 15(b)] and 180 kb in KI (Fig. 22), the signal rises rapidly as the shock approaches the backing electrode, and may reach the conduction signal level before the shock leaves the specimen. This behavior has not been accounted for quantitatively as yet. However, a simple model which treats only the increased conductivity behind the shock (see Appendix B) predicts a monotonically increasing signal as the shock propagates—an even larger signal during most of the transit time than is actually observed. A suitable combination of this treatment with that of Allison and Wenzel might account for the observed effect.

3. Resistivity of Some Insulating Materials

Several insulators have been briefly investigated for suitability as construction materials in conductivity experiments (Table IV). The record shown in Fig. 23 is typical of those obtained. In particular, the signal was often negative after shock transit, which indicates signal generation by the specimen rather than increased conductivity. The ringing observed when the shock reached the electrode-specimen interface is characteristic of the materials tested.

Carbon tetrachloride was included because it was used by Allison and Wenzel in experiments similar to ours. The results of Shot 9379 (Table IV) discouraged its further use.

Of the substances found to be good insulators above 100 kb, silicone oil is considered the most suitable for conducting experiments because of its small conductivity, small polarization, and low viscosity. Hysol and C-7 epoxy are less convenient and exhibit larger polarization signals.

4. Shock Velocities and Determination of Shocked States

The shocked states listed in Tables II and III are only approximate because no state measurements were made. The state in the aluminum driver was assumed known from previous work in this laboratory, and the Hugoniot equation of state data of Christian[25] were used to estimate

Table IV

INSULATION TEST DATA

MATERIAL	SHOCK VELOCITY[a] (mm/μs)	STRESS IN SPECIMEN (kb)	PARTICLE VELOCITY[b] (mm/μs)	SHOT NO.	RESULT[c]
Silastic RTV 932 Dow Corning ρ_0 = 1.05 g/cc	5.1	120	2.24	9477[d]	Material set for 24 hrs; signal after shock transit −0.4 volt; good insulator.
	5.1	120	2.24	9480[d]	Material set for 3 hrs; signal negative after shock transit, < 0.6 volt; good insulator.
Hysol 2039 Epoxy ρ_0 = 1.22 g/cc	5.6	145	2.13	9478[d]	Signal negative after shock transit, < 1.8 volt; good insulator.
Silicone Oil Dow Corning #200 ρ_0 = 0.97 g/cc (3 centistoke)	4.9	108	2.30	9477[d]	Signal after shock transit < +0.4 volt; good insulator..
	5.0	110	2..25	9504[e]	Signal after shock transit < +0.8 volt with no voltage applied.
Arkansas Novaculite ρ_0 = 2.65 g/cc	*f*	~290	~1.5	9481[d]	Signal after shock transit < +0.1 volt; good insulator.
Teflon ρ_0 = 2.2 g/cc	--	~300	--	9237[e]	0.01-in. thick specimen; resistance high, ~10^7 ohm-cm; good insulator.
C-7 Epoxy	5.05	205	1.85	9307[e]	
		~300		9238[e]	0.01-in. thick specimen; $\rho \sim 2 \times 10^4$ ohm-cm; poor insulator at these stress levels.[h]
CCl_4 ρ_0 = 1.59 g/cc	4.92[g]	176[g]	2.26[g]	9379[e]	Signal after shock transit within 8% of short circuit; may be due to polarization or conduction..

[a] Observed from clear-cut polarization signal.

[b] From impedance match solution.

[c] Only positive signal can indicate conduction; power supply voltage ~ −80 volts.

[d] Explosive system, 1½" plane-wave lens + ½" Comp B + ¼" Al driver plate.

[e] Explosive system, 4" plane-wave lens + 2" Comp B + ½" Al driver plate.

[f] No clear-cut polarization signal.

[g] Calculated from unpublished data, Los Alamos Scientific Laboratory.

[h] At ~100 kb, C-7 appears to be good insulator (see Keough, 1963).

graphically the state in the salts. Because of the unexpectedly rapid variation of the conductivity with shock strength, state measurements will be made in future work.

In Table II, both calculated and observed shock velocities are listed. It was found that, in passive (no applied voltage) shots and in low conductivity shots, polarization signals provided a reasonable measure of shock transit time. For some of the shots, where the shock induced conductivity was high, the photomultiplier system described earlier detected shock exits, and the polarization signal indicated shock entrance. These signals were displayed on the two beams of a Type 551 oscilloscope.

With a few exceptions, the agreement between expected and observed velocities is consistent with the rather large uncertainty inherent in the present measurements, where the explosive used was Baratol or Comp B. The TNT shots show greater scatter, presumably due to the poor quality TNT available at shot time.

It should be pointed out that KI under hydrostatic compression undergoes a transition from the sodium chloride structure to the cesium chloride structure at 17.5 kb and room temperature. Christian's data and the present data are consistent with the interpretation that KI is in the high pressure modification at the shock strengths employed in this work.

The temperatures included in Figs. 20 and 21 are those calculated by Christian, assuming C_v and $(\partial P/\partial T)_v$ are constants.

D. DISCUSSION

The lowest resistivity measured for NaCl was greater than 4×10^5 ohm-cm at 274 kb (Table II), whereas Alder[20] and also Al'tshuler *et al.*[10] report values of the range of 10^3 ohm-cm in the same stress range. The reason for the disagreement is not clear, but spuriously low resistivity measurements are more easily rationalized than spuriously high ones.

The measurement techniques used by Alder and Christian are too briefly described in the literature to make detailed comparison possible, although the impression is given that most experiments were performed in a poorly defined transverse geometry. The Russian work, on the other hand, should be directly comparable to our work. The scatter they

observed for crystals from different sources suggests that impurities may be responsible for their relatively high conductivities. Two other possibilities suggest themselves:

1. Polarization signals were mistaken for conductivity signals (it seems strange that no polarization signals were reported by Al'tshuler *et al.*), or
2. The conductivity was due to air trapped at interfaces. The interfaces referred to can also occur within the specimen if it is formed by compressing a powder.

Further work in NaCl should extend the measurements in high-purity crystals to higher shock strengths. Alder has reported a change in slope of the NaCl Hugoniot at about 300 kb (not observed by Al'tshuler *et al.*) which he attributes to a polymorphic transformation to the CsCl structure, similar to the known transitions in other alkali halides. A detailed study of the Hugoniot and the resistivity in this region is desirable.

The results for CsI in both longitudinal and transverse geometries are in reasonable agreement with both Alder and Netherwood.[26] The resistivity decreases more than three orders of magnitude in the vicinity of 230 kb, corresponding to a compression of about 0.64 and temperature of about 3000°K.

For KI, the data from transverse experiments agree best with the results of Alder. Our results indicate that the decrease in resistivity is more gradual for KI than for CsI, in the stress range investigated.

The disagreement between our longitudinal and transverse experiments at low pressure, the transverse indicating the lower resistivities, has not been explained. The possibility that the specimen is electrically anisotropic with respect to the direction of shock propagation cannot be dismissed at this stage of the investigation.

Likewise, the generation of a signal in CsI during shock transit in a transverse experiment with zero applied field has not been explained, but it suggests that anisotropy may exist in a plane perpendicular to the direction of shock propagation.

The conductivity of the alkali halides under shock may be primarily electronic in nature or due to the transport of ions as is true at atmospheric pressure. Electronic conduction might come about by a

polymorphic transformation to a metallic or semimetallic phase. The Hugoniot equation of state has been determined[25] for each of the salts studied with no evidence of a transition occurring in the pressure range of interest. The data do indicate a transition in KI at a lower pressure, but this is believed to correspond to the well-known fcc-bcc transformation observed statically. Furthermore, static resistivity measurements by Drickamer[12] to pressures of the order of 500 kb showed no transition to a conducting phase. Hence the hypothesis of a polymorphic transformation to a conducting phase appears unwarranted.

Alder believes that the conduction is electronic and is made possible by a decrease in the energy gap between valence and conduction bands due to shock compression of the lattice. He infers gap widths of 3 or 4 ev, so that very high temperatures are necessary to achieve significant conduction. This would explain why a static high pressure experiment at room temperature would have a negative result if the pressure did not exceed the shock pressure. However, if Drickamer's pressures were as high as believed and if the band gap continued to decrease with volume at the rate indicated by Alder's interpretation of the Livermore data, a finite resistivity might have been expected for CsI even at room temperature.

Flower and March[27] have calculated the band gap for CsI as a function of isotropic compression of the lattice, and concluded that there is negligible change to 250 kb. To evaluate the accuracy of such a calculation even for hydrostatic compression is difficult, and the effect of strain anisotropy, which is present in the shock case (and perhaps in the static case also), will have to be considered. A further complication is raised by the possibility that extreme disorder prevails behind the shock front.

Ionic conduction is perhaps the most obvious mechanism to consider in trying to explain the observed high conductivities, because conduction at zero pressure is due to the diffusion of ions (or, equivalently, vacancies). Alder rejects this mechanism on the basis that ionic conductivities cannot be as high as observed unless melting occurs. Fusion curves have been obtained by Clark[28] for several alkali halides (not including CsI or KI) up to 25 kb. From a gross extrapolation to shock pressures by means of the Simon equation, Alder concluded that melting points are probably not reached at the pressures attained in present experiments.

The resistivity data reported by Al'tshuler *et al.* for shock stresses above 300 kb in NaCl are in rough agreement* with values expected from extrapolation of the zero-pressure ionic conductivity of NaCl to the calculated shock temperatures. A similar comparison for KI (Fig. 21) indicates even higher conductivities than observed. This extrapolation is only suggestive because, among other things, it ignores the phase transition.

The validity of an extrapolation of fusion data from low to high pressures via the Simon equation can be seriously questioned, as can extrapolation of low temperature, zero-pressure ionic conductivity data to high temperature and to high pressure. It should be noted also that the calculated temperatures are quite uncertain.

For a complete description of ionic transport phenomena in alkali halide crystals, the reader is referred to Chapter 2 in Mott and Gurney[29] or Chapter 17 in Kittel.[30] Briefly, the intrinsic ionic resistivity† in alkali halide crystals depends on temperature T as

$$\rho = \frac{kT}{N_0 e^2 p \nu \alpha^2} \tag{3}$$

where k is Boltzmann's constant, N_0 the total number of ions per unit volume of charge e, p the proportion of charge carriers, ν the thermally induced ionic vibration frequency, and α the lattice spacing. Alkali halide transference number measurements have shown that cation transport accounts for perhaps 90% of the conductivity.[29] The jump frequency for cation-cation vacancy interchange (the dominant mechanism) is then given as

$$\nu = \nu_0^+ \exp\ (-\epsilon/kT) \tag{4}$$

where ϵ is the barrier activation energy. The proportion of positive ion vacancies at *equilibrium* is given by

$$p \cong \exp\ (-\epsilon'/2kT) \tag{5}$$

*At lower pressures the agreement is less certain.

†The salt will exhibit intrinsic conductivity when the equilibrium number of thermally activated, positive ion vacancies is much larger than the number of divalent impurity cations.

where ϵ' is the activation energy for the formation of both an anion and cation vacancy (formation of this combination rather than single vacancies is energetically favored). The equilibrium intrinsic ionic resistivity is given by substitution of Eqs. (4) and (5) into (3).

In the case of a shocked crystal it is almost certain that the equilibrium number of vacancies appropriate to the shock temperature is *not* given by Eq. (3). It is presently unclear whether, upon shocking, the vacancy concentration increases or decreases. Because of this uncertainty, the agreement between Al'tshuler's data and the extrapolation of the zero-pressure ionic conductivity data for NaCl could be fortuitous.

E. CONCLUSIONS

1. The resistivity of NaCl at 231 kb is greater than approximately 4×10^5 ohm-cm.

2. The resistivity of CsI decreases from greater than 10^7 ohm-cm at 100 kb to less than 1 ohm-cm at 274 kb. The resistivity decreases rapidly from 10^5 to 10^2 ohm-cm at a compression of 0.64 (~200 kb), in fair agreement with the result of Alder.

3. The resistivity of KI decreases from greater than 10^5 ohm-cm at 100 kb to less than 1 ohm-cm at 233 kb in the longitudinal geometry. A rapid decrease from 10^4 ohm-cm at 181 kb to 10^2 ohm-cm at 196 kb (±10 kb) has been observed, compared to a value between 50 and 150 ohm-cm at 160 kb reported by Alder.

4. In addition to considering the conduction mechanism as being due to a decrease in band gap with compression, as suggested by Alder, the hypothesis that ionic conduction in the solid may account for the observed conductivity must also be critically considered.

5. Signals are generated during the propagation of shock fronts through alkali halide crystals in longitudinal geometry.

6. In a longitudinal geometry experiment utilizing the measuring circuit described in this report, a signal is to be expected as the shock traverses the specimen if it causes the material to become conducting. A simple model of the specimen as a variable parallel plate capacitor was considered, but the calculated signal was not in quantitative agreement with that observed.

APPENDIX A

DETERMINATION OF RESISTIVITY FROM A TRANSVERSE GEOMETRY EXPERIMENT

APPENDIX A

DETERMINATION OF RESISTIVITY FROM A TRANSVERSE GEOMETRY EXPERIMENT

Consider a shock of velocity U_1 incident on a specimen of thickness c_0 and specific volume V_0. The mechanical state of the shocked material is determined by the specific volume V_1 and particle velocity u_1. The initial traverse of the specimen requires the time

$$t_1 = \frac{c_0}{U_1} \quad .$$

If the backing block is a good impedance match to the specimen, a quasi steady-state stress condition will exist in the specimen for a short time after $t = t_1$. The resistivity then is simply calculable using Eq. (2) of Section II-B, taking into account the decrease in conduction area, A, produced by the shock compression. When the specimen and backing plate are mismatched in impedance, the resistivity may be obtained from the voltage V_x at a specific time, or from the functional dependence of V_x on time discussed below (see typical record of signal obtained in transverse geometry in Fig. A-1). If the initial specimen resistivity is assumed to be infinite, at a time t such that

$$0 \leq t < t_1 \quad ,$$

the resistivity ρ_A behind the shock (Fig. A-2) may be expressed in terms of the observed voltage V_x by

$$\frac{a\rho_A}{b(U_1 - u_1)t} = R_0\left(\frac{V_0}{V_x} - 1\right) \quad . \qquad \text{(A-1)}$$

Equation (A-1) is obtained from Eq. (2) by explicitly expressing the time dependence of the area of conduction. Differentiating Eq. (A-1) with respect to t results in

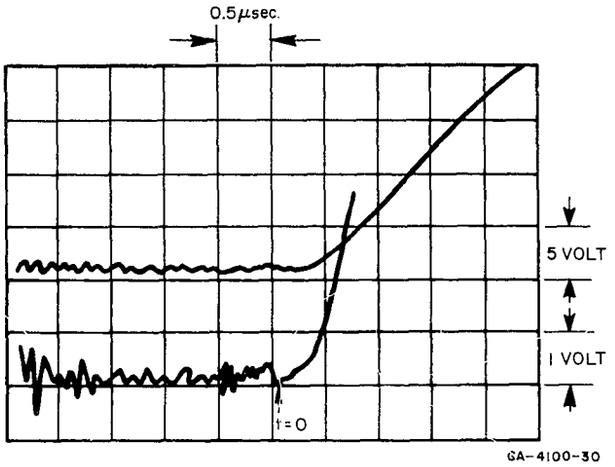

FIG. A-1 CONDUCTION SIGNAL FOR CsI AT 215 kb – TRANSVERSE GEOMETRY, SHOT 9517

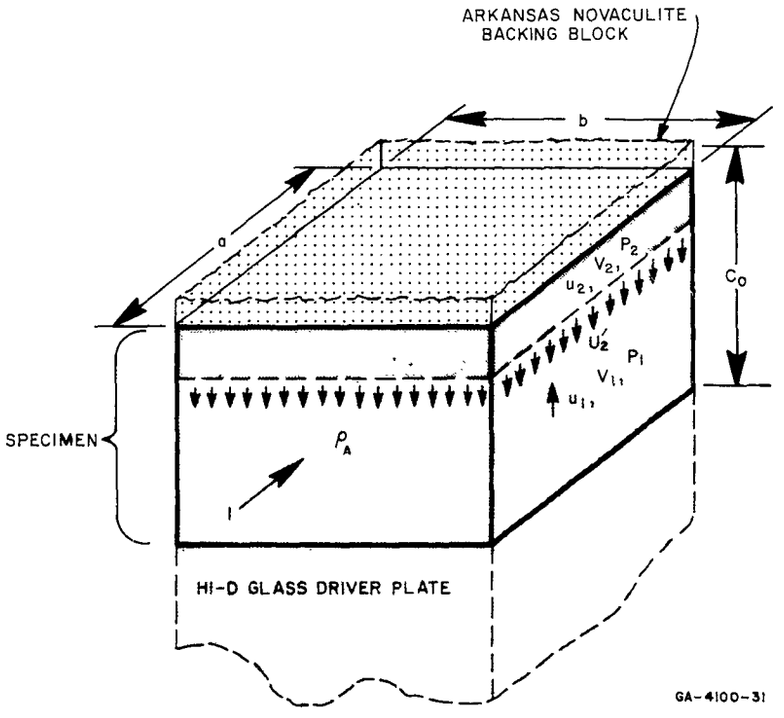

FIG. A-2 PARAMETERS DESCRIBING STRESS, VOLUME, AND RESISTIVITY IN REFLECTED STATE ACHIEVED IN TRANSVERSE GEOMETRY EXPERIMENT

$$\frac{\partial V_x}{\partial t} = \frac{bR_0V_0}{a\rho_A}(U_1 - u_1)\left(1 - \frac{V_x}{V_0}\right)^2 \quad . \tag{A-2}$$

Equation (A-2) allows the determination of ρ_A from the amplitude and slope of the observed signal. Note that if $V_x << V_0$ for a sufficiently long time, V_x varies linearly with t, and ρ_A may be determined from the slope alone.

When the incident shock reaches the backing block, a reflected shock or rarefaction wave (Fig. A-2) is propagated back into the specimen with velocity U_2' and brings the material behind it to a specific volume V_2, particle velocity u_2, stress P_2, and resistivity ρ_B (velocities in laboratory coordinates). This reflected wave will traverse the specimen in time

$$t_2 = c_0(U_1 - u_1)/[U_1(U_2' + u_1)] \quad .$$

By considering the material on both sides of the reflected wave, of resistivity ρ_A and ρ_B, in a parallel circuit, the resistivity in the time interval $t_1 \leq t \leq t_2$ may be written as

$$\frac{b}{a}\left\{\frac{[(U_1 - u_1)t_1 - (u_1 + U_2')(t - t_1)]}{\rho_A} + \frac{(u_2 + U_2')(t - t_1)}{\rho_B}\right\} = \left[R_0\left(\frac{V_0}{V_x} - 1\right)\right]^{-1} \quad . \tag{A-3}$$

Differentiation results in

$$\frac{b}{a}\left[-\frac{(u_1 + U_2')}{\rho_A} + \frac{(u_2 + U_2')}{\rho_B}\right] = \frac{1}{R_0V_0}\left(1 - \frac{V_x}{V_0}\right)^{-2}\left(\frac{\partial V_x}{\partial t}\right) \quad . \tag{A-4}$$

Equation (A-4) can be solved for ρ_B in terms of signal slope and amplitude and, of course, ρ_A. Again, if $V_x << V_0$, the slope is constant and ρ_B is given by

$$\rho_B \cong \frac{u_2 + U_2'}{\frac{a}{bV_0R_0}\left(\frac{\partial V_x}{\partial t}\right) + \frac{u_1 + U_2'}{\rho_A}} \quad . \tag{A-5}$$

APPENDIX B

A VARIABLE CAPACITOR MODEL OF A SPECIMEN IN A LONGITUDINAL GEOMETRY EXPERIMENT

APPENDIX B

A VARIABLE CAPACITOR MODEL OF A SPECIMEN IN A LONGITUDINAL GEOMETRY EXPERIMENT

It is instructive to consider the specimen as represented by a variable parallel plate capacitor—C_1 in Fig. B-1. The fixed plate of C_1 corresponds to the backing electrode, and the moving plate corresponds to the shock front; the area A of C_1 is assumed constant. The material behind the shock front is taken, for the present, to have zero

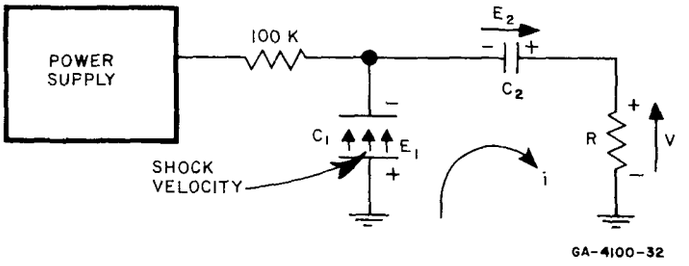

FIG. B-1 CIRCUIT SCHEMATIC APPROPRIATE TO VARIABLE CAPACITOR MODEL OF SHOCKED SPECIMEN

resistivity. The 2-μf capacitor of Fig. 12 is represented by C_2 in Fig. B-1, and R represents the lumped impedance (resistive) of the RG71 cable with a 91-ohm resistor at each end. For this circuit, the initial conditions at time $t = 0$ may be stated as

$$
\begin{aligned}
E_1(0) &= E_2(0) = V_0 \quad , && \text{(a)} \\
Q_1(0) &= \frac{V_0 A \epsilon}{c_0} \quad , && \text{(b)} \\
Q_2(0) &= V_0 C_2 \quad , \quad \text{and} && \text{(c)} \\
i(0) &= 0 \quad , && \text{(d)}
\end{aligned}
\qquad \text{(B-1)}
$$

where V_0 is the power supply voltage, $Q_1(t)$ and $Q_2(t)$ are the charges on the capacitors C_1 and C_2. In Eq. [B-1(b)], the infinite parallel plate capacitor formula is assumed for simplicity in which A is the capacitor area, c_0 the thickness, and ϵ the electrical permittivity of the unshocked specimen.

Consider the effect of suddenly short-circuiting C_1 with the power supply voltage on. The voltage E_2 will decay with the time constant RC_2 which, for the component values given in Fig. 12, is 90 μsec. Because this time is long compared to the time of shock wave traversal of the specimen, it is assumed that

$$E_2 = V_0 = \text{constant} \quad . \tag{B-2}$$

Kirchoff's law states that

$$V - E_2 + E_1 = 0$$

which, using Eq. (B-2), may be written

$$V = V_0 - \frac{Q_1(t)}{C_1(t)} \quad . \tag{B-3}$$

If the instantaneous current is i, conservation of charge gives

$$Q_1(t) = Q_1(0) + \int_0^t i\,dt = \frac{V_0 A\epsilon}{c_0} + \int_0^t i\,dt \quad , \tag{B-4}$$

while the proposition that the shock front represents the moving plate of a capacitor implies

$$C_1 = \frac{A\epsilon}{c_0 - U_1 t} \tag{B-5}$$

where U_1, as before, is the shock velocity. Substitution of Eqs. (B-4) and (B-5) into Eq. (B-3) leads to the result*

$$i = \frac{V_0}{R}\left[1 - (c_0 - U_1 t)\left(\frac{1}{c_0} + \frac{1}{V_0 A\epsilon}\int_0^t i\,dt\right)\right] \qquad (B-6)$$

for $0 \leq t \leq c_0/U_1$.

Using the trapezoidal approximation to expand the integral, i may be numerically evaluated. A small time increment Δt is defined so that

$$t_n = n\Delta t \quad .$$

The current $i = i_n$ at time $t = t_n$ may then be written as

$$i_n = \frac{2A\epsilon V_0}{2RA\epsilon + (c_0 - U_1 t_n)\Delta t}\left\{1 - (c_0 - U_1 t_n)\left[\frac{1}{c_0} + \frac{\Delta t}{2A\epsilon V_0}\,(i_0 + 2i_1 + 2i_2 + \ldots + 2i_{n-1})\right]\right\} \qquad (B-7)$$

The effect of a nonzero resistivity ρ_A of the material behind the shock front may be included by writing in place of Eq. (B-3)

$$V = V_0 - \left[\frac{Q_1(t)}{C_1(t)} + \frac{\rho_A(U_1 - u_1)\,it}{A}\right] \quad . \qquad (B-8)$$

---

* An explicit relation for $i(t)$ can be obtained by substituting RdQ_1/dt for V in Eq. (B-3), solving for Q_1, and differentiating to get i. Writing C_1^0 for C_1 at $t = 0$, the result is

$$i = \frac{V_0}{R}\left\{1 - e^{-\frac{1}{RC_1^0}\left(1-\frac{t}{2t_1}\right)}\left[1 + \frac{1}{RC_1^0}\left(1 - \frac{t}{t_1}\right)\int_0^t e^{\frac{t}{RC_1^0}\left(1-\frac{t}{2t_1}\right)}\,dt\right]\right\}$$

An expression analogous to Eq. (B-6), with R replaced by $R + \rho_A(U_1 - u_1)t/A$, is then obtained which yields i_n upon numerical evaluation of

$$i_n = \frac{2A\epsilon V_0\left\{1 - (c_0 - U_1 t_n)\left[\frac{1}{c_0} + \frac{\Delta t(i_0 + 2i_1 + 2i_2 + \ldots 2i_{n-1})}{2A\epsilon V_0}\right]\right\}}{2A\epsilon R + c_0\Delta t + [U_1(2\epsilon\rho_A - \Delta t) - 2u_1\epsilon\rho_A]t_n} \qquad \text{(B-9)}$$

Equation (B-9) has been evaluated on a Burroughs 220 Computer for what is assumed to be a realistic set of constants for shock propagation in *KI*. The numerical values used are listed below:

$$\epsilon = 4.96 \times 10^{-13} \text{ farads/cm}$$

$$A = 1.98 \text{ cm}^2$$

$$\rho_A = 3 \text{ ohm-cm}$$

$$V_0 = 90 \text{ volts}$$

$$\left.\begin{aligned} c_0 &= 0.329 \text{ cm} \\ U_1 &= 0.426 \times 10^6 \text{ cm/sec} \end{aligned}\right\} t_1 = \frac{c_0}{U_1} = 7.72 \times 10^{-7} \text{ sec}$$

$$u_1 = 0.178 \times 10^6 \text{ cm/sec}$$

This gives the somewhat surprising result that the current is nearly linearly related to the time (Fig. B-2). The solution passes through the proper end points (0,0) and

$$t_1 , \left(\frac{V_0}{R + \rho_A \dfrac{c_0(U_1 - u_1)}{U_1 A}}\right) .$$

The addition of the nonzero resistivity causes a negligible effect because the maximum specimen resistance is small compared with R.

The calculated curve has the general shape which is experimentally observed (Figs. 15 and 22), but predicts far too great current at all times except $t = 0$ and $t \cong t_1$. This result is suggestive that another current-retarding mechanism, aside from resistivity, should be included in further refinement of this treatment.

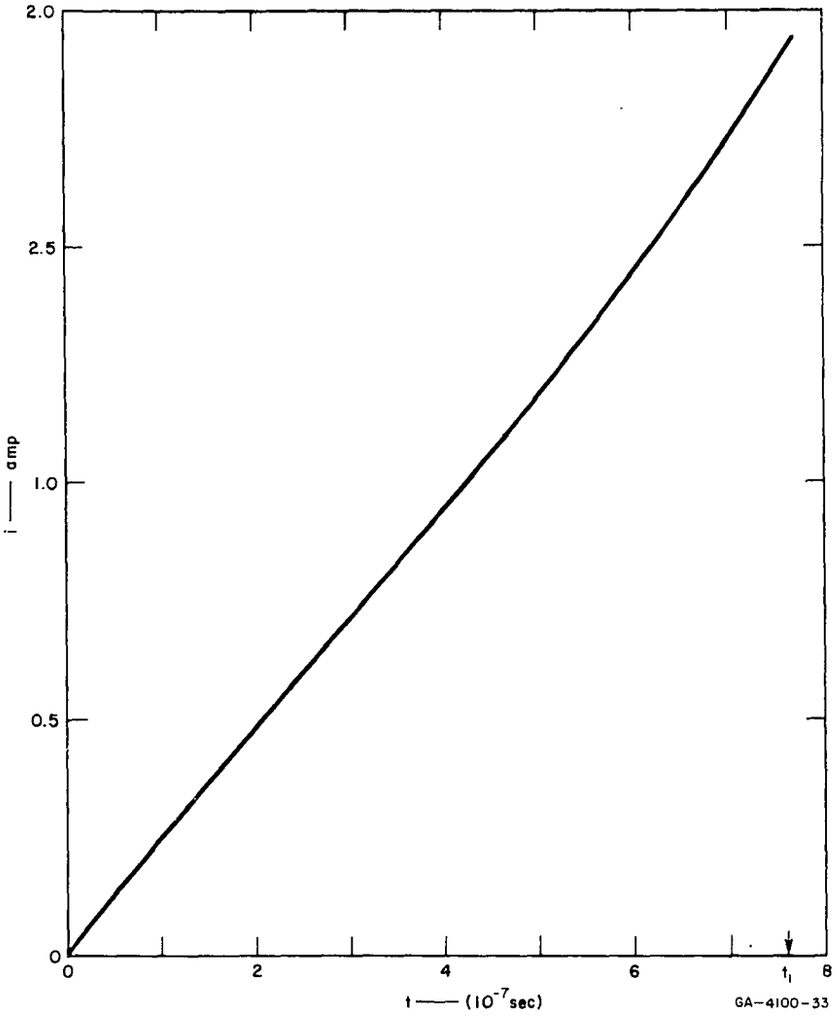

FIG. B-2 CURRENT vs. TIME FOR VARIABLE CAPACITOR MODEL OF KI AT 233 kb. Resistivity of Shocked Region Assumed to be 3 ohm-cm

ACKNOWLEDGMENTS

The thermoelectric experiments were carried out by Donald Hartill. William Wilkinson assisted in some of the resistivity measurements. Helpful discussions with Weston Farrand, Douglas Keough, and Drs. John Jamieson, David Bernstein, and George Duvall are gratefully acknowledged.

REFERENCES

1. Doran, D. G., unpublished report.

2. Minshall, S., private communication.

3. Jacquesson, J., "Contribution a l'Etude de la Propagation et des Ondes de Choc dans les Metaux," doctoral thesis, University of Poitiers, France, April 1962. See also: "Etude du Profil des Ondes de Choc dans Quelques Metaux," *Les Ondes de Detonation*, Editions du Centre National de la Recherche Scientifique, 15 Quai Anatole-France-Paris (VII^{e}), 415-422 (1962).

4. Ilyukhin, V. S. and V. N. Kologrivov, "EMF in Thermocouples Compressed by Shock Waves," Abstr. *Curr. Rev. Sov. Tech. Press*, p. 1 (856) (Dec. 21, 1962), *Zhurnal prikladnoy mekhaniki i tekhnicheskoy fiziki*, **5**, 175-6 (1962).

5. Alder, B. J., and R. H. Christian, "Metallic Transition in Ionic and Molecular Crystals," *Phys. Rev.* **104**, 550-551 (1956).

6. Brish, A. A., M. S. Tarasov and V. A. Tsukerman, "Electrical Conductivity of Dielectrics in Strong Shock Waves," *Soviet Physics JETP* **11**, 15-17 (1960).

7. David, H. G., and S. O. Hamman, "Sulfur: A Possible Metallic Form," *J. Chem. Phys.* **28**, 1006 (1958), Letter.

8. Joigneau, S. and J. Thouvenin, "Electrical Conductivity of Sulfur under the Action of a Shock Wave," *C. R. Acad. Sci.* (Paris) **246**, 3422-3425 (1958).

9. Hauver, G. E., "Pressure Profiles in Detonating Solid Explosive," Third Symposium on Detonation, ONR Symposium Report ACR-52, Vol. 1, 241-252 (1960).

10. Al'tshuler, L. V., L. V. Kuleshova, and M. N. Pavlovskii, "The Dynamic Compressibility, Equation of State, and Electrical Conductivity of Sodium Chloride at High Pressures," *Soviet Physics JETP* **12**, 10-15 (1961).

11. Fuller, P. J. A. and J. H. Price, "Electrical Conductivity of Manganin and Iron at High Pressure," *Nature* **193**, 262-263 (1962).

12. Drickamer, H. G., private communication.

13. Taylor, J. W., "Residual Temperatures of Shocked Copper," *J. Appl. Phys.* **34**, 2727-2731 (1963); also, McQueen, R. G., private communication.

14. Walsh, J. M., M. H. Rice, R. G. McQueen, and F. L. Yarger, "Shock-Wave Compression of Twenty-Seven Metals. Equations of State of Metals," *Phys. Rev.* **108**, 196-216 (1957).

15. Bundy, F. P. and H. M. Strong, "Behavior of Metals at High Temperature and Pressure," *Solid State Physics*, Seitz and Turnbull, eds., Academic Press, New York, 1962, Vol. 13, p. 140.

16. Bancroft, D., E. L. Peterson, and S. Minshall, "Polymorphism of Iron at High Pressure," *J. Appl. Phys.* **27**, 291-8 (1956).

17. Ziman, J. M., *Electrons and Phonons*, Oxford Univ. Press, London, 1960, p. 397.

18. Thomson, Robb, private communication.

19. McQueen, R. G. and S. P. Marsh, "Equation of State for Nineteen Metallic Elements from Shock-Wave Measurements to Two Megabars," *J. Appl. Phys.* **31**, 1253-69 (1960).

20. Alder, B. J., "Physics Experiments with Strong Pressure Pulses," *Solids under Pressure*, W. Paul and D. M. Warshauer, eds., McGraw Hill, New York, 1963, pp. 385-420.

21. Eichelberger, R. J. and G. E. Hauver, "Solid State Transducers for Recording of Intense Pressure Pulses," *Les Ondes de Detonation*, Editions de Centre National de la Recherche Scientifique, 15 Quai Anatole-France-Paris (VII^{e}), 363-381 (1962).

22. Hikata, A., C. Elbaum, B. Chick, and R. Truell, "Electrical-Charge Study in Sodium Chloride During Plastic Deformation," *J. Appl. Phys.* **34**, 2154-2158 (1963).

23. Keough, D., "Pressure Transducer for Measuring Shock Wave Profiles," Final Rpt. Stanford Research Institute, Project 3713, 1963.

24. Allison, F. E. and A. B. Wenzel, "The Shock-Induced Polarization of Dielectrics," BRL Mem. Rpt. No. 1449, 1962.

25. Christian, R. H., "The Equation of State of the Alkali Halides at High Pressure," doctoral thesis, University of California, 1957, p. 89.

26. Netherwood, P., private communication.

27. Flower, M. and N. H. March, "Transitions to Metallic States in Ionic Crystals, with Particular Reference to Cesium Iodide," *Phys. Rev.* **125**, 1144-1146 (1962).

28. Clark, S. B., Jr., "Effect of Pressure on the Melting Points of Eight Alkali Halides," *J. Chem. Phys.* **31**, 1526-1531 (1959).

29. Mott, M. and R. Gurney, *Electronic Processes in Ionic Crystals,* Oxford University Press, London, 2nd Ed., pp. 275.

30. Kittel, C., *Introduction to Solid State Physics,* 2nd Ed., John Wiley and Sons, Inc., New York, 1956, p. 617.

31. Lehfeldt, W., "Uber die elektrische Leitfahigkeit von Einkristallen," *Zeits. f. Physik* **85**, 717-726 (1933).

32. Gregson, V. G., T. J. Ahrens, and C. F. Peterson, "Dynamic Properties of Rocks," Final Rpt. Stanford Research Institute Project 3630, 1963.

STANFORD RESEARCH INSTITUTE, Menlo Park, California

Final Report PGU-4100, ELECTRICAL EFFECTS OF SHOCK WAVES: CONDUCTIVITY IN CsI AND KI. THERMOELECTRIC MEASUREMENTS IN METALS. August 1963, 54 pp. incl. 30 illus., tables. Unclassified Report

Incidence of a 400 kb shock wave in copper upon a constantan probe produces a peak emf of the order of 80 mv, compared with 14 mv calculated from zero-pressure thermopowers and theoretical shock temperatures. At 170 kb, measured peak emfs range from 23 to 90 mv, compared with 4 mv calculated similarly. The signals decrease by 50% during first 0.1 to 0.3 μsec followed by a much less rapid decrease. Partial diffusion welding of junction reduces initial spike at 400 kb. Varying probe diameter from 1/8 inch to 3/4 inch only slightly affects signal. Anomalously high emfs are also observed with aluminum-constantan, copper-iron, and copper-aluminum junctions. Signal amplitudes are related approximately as they would be at zero pressure, with the exception of copper-iron in which the iron is known to undergo a phase transition.

Electrical resistivities of single crystal NaCl, KI, and CsI have been measured at several shock pressures in the range 84 to 274 kb. The resistivity of

UNCLASSIFIED

1. Shock Waves
2. Metals
3. Resistivity
4. Alkali Halides
5. Thermoelectric

I Contract DA-04-200-ORD-1279

II D. G. Doran, T. J. Ahrens

STANFORD RESEARCH INSTITUTE, Menlo Park, California

Final Report PGU-4100, ELECTRICAL EFFECTS OF SHOCK WAVES: CONDUCTIVITY IN CsI AND KI. THERMOELECTRIC MEASUREMENTS IN METALS. August 1963, 54 pp. incl. 30 illus., tables. Unclassified Report

Incidence of a 400 kb shock wave in copper upon a constantan probe produces a peak emf of the order of 80 mv, compared with 14 mv calculated from zero-pressure thermopowers and theoretical shock temperatures. At 170 kb, measured peak emfs range from 23 to 90 mv, compared with 4 mv calculated similarly. The signals decrease by 50% during first 0.1 to 0.3 μsec followed by a much less rapid decrease. Partial diffusion welding of junction reduces initial spike at 400 kb. Varying probe diameter from 1/8 inch to 3/4 inch only slightly affects signal. Anomalously high emfs are also observed with aluminum-constantan, copper-iron, and copper-aluminum junctions. Signal amplitudes are related approximately as they would be at zero pressure, with the exception of copper-iron in which the iron is known to undergo a phase transition.

Electrical resistivities of single crystal NaCl, KI, and CsI have been measured at several shock pressures in the range 84 to 274 kb. The resistivity of

UNCLASSIFIED

1. Shock Waves
2. Metals
3. Resistivity
4. Alkali Halides
5. Thermoelectric

I Contract DA-04-200-ORD-1279

II D. G. Doran, T. J. Ahrens

STANFORD RESEARCH INSTITUTE, Menlo Park, California

Final Report PGU-4100, ELECTRICAL EFFECTS OF SHOCK WAVES: CONDUCTIVITY IN CsI AND KI. THERMOELECTRIC MEASUREMENTS IN METALS. August 1963, 54 pp. incl. 30 illus., tables. Unclassified Report

Incidence of a 400 kb shock wave in copper upon a constantan probe produces a peak emf of the order of 80 mv, compared with 14 mv calculated from zero-pressure thermopowers and theoretical shock temperatures. At 170 kb, measured peak emfs range from 23 to 90 mv, compared with 4 mv calculated similarly. The signals decrease by 50% during first 0.1 to 0.3 μsec followed by a much less rapid decrease. Partial diffusion welding of junction reduces initial spike at 400 kb. Varying probe diameter from 1/8 inch to 3/4 inch only slightly affects signal. Anomalously high emfs are also observed with aluminum-constantan, copper-iron, and copper-aluminum junctions. Signal amplitudes are related approximately as they would be at zero pressure, with the exception of copper-iron in which the iron is known to undergo a phase transition.

Electrical resistivities of single crystal NaCl, KI, and CsI have been measured at several shock pressures in the range 84 to 274 kb. The resistivity of

UNCLASSIFIED

1. Shock Waves
2. Metals
3. Resistivity
4. Alkali Halides
5. Thermoelectric

I Contract DA-04-200-ORD-1279

II D. G. Doran, T. J. Ahrens

STANFORD RESEARCH INSTITUTE, Menlo Park, California

Final Report PGU-4100, ELECTRICAL EFFECTS OF SHOCK WAVES: CONDUCTIVITY IN CsI AND KI. THERMOELECTRIC MEASUREMENTS IN METALS. August 1963, 54 pp. incl. 30 illus., tables. Unclassified Report

Incidence of a 400 kb shock wave in copper upon a constantan probe produces a peak emf of the order of 80 mv, compared with 14 mv calculated from zero-pressure thermopowers and theoretical shock temperatures. At 170 kb, measured peak emfs range from 23 to 90 mv, compared with 4 mv calculated similarly The signals decrease by 50% during first 0.1 to 0.3 μsec followed by a much less rapid decrease. Partial diffusion welding of junction reduces initial spike at 400 kb. Varying probe diameter from 1/8 inch to 3/4 inch only slightly affects signal. Anomalously high emfs are also observed with aluminum-constantan, copper-iron, and copper-aluminum junctions. Signal amplitudes are related approximately as they would be at zero pressure, with the exception of copper-iron in which the iron is known to undergo a phase transition.

Electrical resistivities of single crystal NaCl, KI, and CsI have been measured at several shock pressures in the range 84 to 274 kb. The resistivity of

UNCLASSIFIED

1. Shock Waves
2. Metals
3. Resistivity
4. Alkali Halides
5. Thermoelectric

I Contract DA-04-200-ORD-1279

II D. G. Doran, T. J. Ahrens

NaCl is greater than 4 x 10^5 ohm-cm at 231 kb, in disagreement with both Alder (*Solids Under Pressure*, McGraw Hill, N.Y., 1963, pp. 385-420) and Al'tshuler *et al* (*Soviet Physics JETP, 12*, 10-15 (1961)). The resistivity of KI is greater than 2 x 10^5 ohm-cm at 93 kb, but drops to less than 1 ohm-cm at 233 kb. The resistivity of CsI is greater than 6 x 10^5 ohm-cm at 215 kb, and less than 25 ohm-cm at 274 kb. Agreement with Alder for CsI and KI is semiquantitative. Resistivity measurements were performed parallel (longitudinal geometry) and perpendicular (transverse geometry) to the shock propagation direction; the above values are for longitudinal geometry. The few measurements in transverse geometry indicate lower resistivities, particularly for KI. In longitudinal geometry a signal is produced during shock transit which, if the shocked specimen resistivity is high, is independent of applied voltage and is qualitatively similar to that observed in insulators by Hauver (ONR Symposium Report ACR-52, Vol. 1, 241-252 (1960)). If the resistivity of the shocked material is low, the signal observed is not that predicted on the basis of low resistivity alone.	UNCLASSIFIED	NaCl is greater than 4 x 10^5 ohm-cm at 231 kb, in disagreement with both Alder (*Solids Under Pressure*, McGraw Hill, N.Y., 1963, pp. 385-420) and Al'tshuler *et al* (*Soviet Physics JETP, 12*, 10-15 (1963)). The resistivity of KI is greater than 2 x 10^5 ohm-cm at 93 kb, but drops to less than 1 ohm-cm at 233 kb. The resistivity of CsI is greater than 6 x 10^5 ohm-cm at 215 kb, and less than 25 ohm-cm at 274 kb. Agreement with Alder for CsI and KI is semiquantitative. Resistivity measurements were performed parallel (longitudinal geometry) and perpendicular (transverse geometry) to the shock propagation direction; the above values are for longitudinal geometry. The few measurements in transverse geometry indicate lower resistivities, particularly for KI. In longitudinal geometry a signal is produced during shock transit which, if the shocked specimen resistivity is high, is independent of applied voltage and is qualitatively similar to that observed in insulators by Hauver (ONR Symposium Report ACR-52, Vol. 1, 241-252 (1960)). If the resistivity of the shocked material is low, the signal observed is not that predicted on the basis of low resistivity alone.	UNCLASSIFIED
NaCl is greater than 4 x 10^5 ohm-cm at 231 kb, in disagreement with both Alder (*Solids Under Pressure*, McGraw Hill, N.Y., 1963, pp. 385-420) and Al'tshuler *et al* (*Soviet Physics JETP, 12*, 10-15 (1961)). The resistivity of KI is greater than 2 x 10^5 ohm-cm at 93 kb, but drops to less than 1 ohm-cm at 233 kb. The resistivity of CsI is greater than 6 x 10^5 ohm-cm at 215 kb, and less than 25 ohm-cm at 274 kb. Agreement with Alder for CsI and KI is semiquantitative. Resistivity measurements were performed parallel (longitudinal geometry) and perpendicular (transverse geometry) to the shock propagation direction; the above values are for longitudinal geometry. The few measurements in transverse geometry indicate lower resistivities, particularly for KI. In longitudinal geometry a signal is produced during shock transit which, if the shocked specimen resistivity is high, is independent of applied voltage and is qualitatively similar to that observed in insulators by Hauver (ONR Symposium Report ACR-52, Vol. 1, 241-252 (1960)). If the resistivity of the shocked material is low, the signal observed is not that predicted on the basis of low resistivity alone.	UNCLASSIFIED	NaCl is greater than 4 x 10^5 ohm-cm at 231 kb, in disagreement with both Alder (*Solids Under Pressure*, McGraw Hill N.Y., 1963, pp. 385-420) and Al'tshuler *et al* (*Soviet Physics JETP, 12*, 10-15 (1961)). The resistivity of KI is greater than 2 x 10^5 ohm-cm at 93 kb, but drops to less than 1 ohm-cm at 233 kb. The resistivity of CsI is greater than 6 x 10^5 ohm-cm at 215 kb, and less than 25 ohm-cm at 274 kb. Agreement with Alder for CsI and KI is semiquantitative. Resistivity measurements were performed parallel (longitudinal geometry) and perpendicular (transverse geometry) to the shock propagation direction; the above values are for longitudinal geometry. The few measurements in transverse geometry indicate lower resistivities, particularly for KI. In longitudinal geometry a signal is produced during shock transit which, if the shocked specimen resistivity is high, is independent of applied voltage and is qualitatively similar to that observed in insulators by Hauver (ONR Symposium Report ACR-52, Vol. 1, 241-252 (1960)). If the resistivity of the shocked material is low, the signal observed is not that predicted on the basis of low resistivity alone.	UNCLASSIFIED

STANFORD
RESEARCH
INSTITUTE

MENLO PARK
CALIFORNIA

Regional Offices and Laboratories

Southern California Laboratories
820 Mission Street
South Pasadena, California

Washington Office
808–17th Street, N.W.
Washington 6, D.C.

New York Office
270 Park Avenue, Room 1770
New York 17, New York

Detroit Office
1025 East Maple Road
Birmingham, Michigan

European Office
Pelikanstrasse 37
Zurich 1, Switzerland

Japan Office
c/o Nomura Securities Co., Ltd.
1–1 Nihonbashidori, Chuo-ku
Tokyo, Japan

Representatives

Toronto, Ontario, Canada
Cyril A. Ing
Room 710, 67 Yonge St.
Toronto 1, Ontario, Canada

Milan, Italy
Lorenzo Franceschini
Via Macedonio Melloni, 49
Milano, Italy

UNCLASSIFIED